

A Peroxynitrite Dicopper Complex: Formation via Cu–NO and Cu–O₂ Intermediates and Reactivity via O–O Cleavage Chemistry

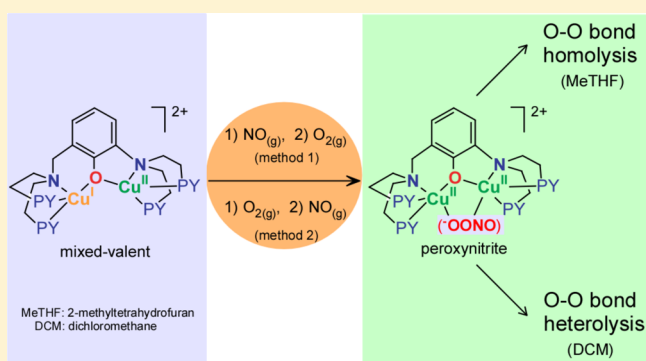
Rui Cao,[†] Lee Taylor Elrod,[‡] Ryan L. Lehane,[‡] Eunsuk Kim,[‡] and Kenneth D. Karlin^{*,†}

[†]Department of Chemistry, Johns Hopkins University, Baltimore, Maryland 21218, United States

[‡]Department of Chemistry, Brown University, Providence, Rhode Island 02912, United States

S Supporting Information

ABSTRACT: A mixed-valent Cu(I)Cu(II) complex, [Cu^{I,II}₂(UN-O⁻)]²⁺ (1), reacts with NO_(g) at -80 °C to form [Cu^{I,II}₂(UN-O⁻)(NO)]²⁺ (2), best described as a mixed-valent nitrosyl complex that has a ν(N–O) band at 1670 cm⁻¹ in its infrared (IR) spectrum. Complex 2 undertakes a one-electron oxidation via the addition of O_{2(g)} to generate a new intermediate, best described as a superoxide and nitrosyl adduct, [Cu^{II,III}₂(UN-O⁻)(NO)(O₂⁻)]²⁺ (3), based on its distinctively blue-shifted ν(N–O) band at 1853 cm⁻¹. Over the course of 20 min at -80 °C, 3 is converted to the peroxynitrite (PN) complex [Cu^{II,III}₂(UN-O⁻)(⁻OOON=O)]²⁺ (4), which was characterized by low-temperature electrospray ionization mass spectrometry (ESI-MS) and IR spectroscopy; ν(N–O) absorptions at 1520 and 1640 cm⁻¹ have been assigned as *cis*- and *trans*-conformers of the PN ligand in 4. Alternatively, the superoxide complex [Cu^{II,III}₂(UN-O⁻)(O₂^{•-})]²⁺ (5) is found to react with NO_(g) to generate the same intermediate superoxide and nitrosyl adduct 3 (based on IR criteria), which likewise converts to the same PN complex 4. The O–O bond in 4 undergoes heterolysis in dichloromethane solvent and is postulated to produce nitronium ion, leading to *ortho*-nitration of 2,4-di-*tert*-butylphenol (DTBP). However, in 2-methyltetrahydrofuran as solvent, the O–O bond undergoes homolysis to generate [•]NO₂ (detected spectrophotometrically) and a putative higher-valent complex, [Cu^{IV,III}₂(UN-O⁻)(O²⁻)]²⁺, that abstracts a H-atom from DTBP to give [Cu^{II,III}₂(UN-O⁻)(OH)]²⁺ and a phenoxyl radical. The latter may dimerize to form the bis-phenol observed experimentally or couple with the [•]NO₂ present, leading to *o*-phenol nitration.

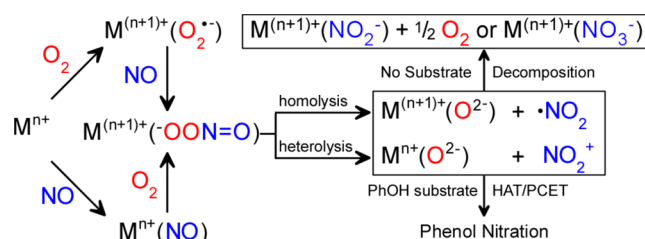


INTRODUCTION

Over 10¹³ oxygen molecules (i.e., dioxygen, O₂) are consumed in a single human cell per day,¹ about 1% of which become free (unbound) radicals, i.e., reactive oxygen species (ROS) and/or reactive nitrogen species (RNS) including superoxide, hydroxyl radical, and peroxynitrite (PN; ⁻OOON=O).^{1b} In biology, PN is commonly proposed to be responsible for tyrosine nitration, which may lead to loss of protein function and/or other deleterious consequences.² PN may be generated from the very fast coupling of superoxide radical (O₂^{•-}) with nitric oxide (NO; nitrogen monoxide);³ the latter itself plays a key role in a variety of biological processes, including signaling, neural transmission, and the immune system.⁴ Superoxide concentrations in cells are limited by superoxide dismutases (Zn/CuSOD and MnSOD), converting 2O₂^{•-} to H₂O₂ and O₂, thereby suppressing PN production.⁵

Extensive biomolecule (e.g., protein Tyr residues, lipids) nitration and/or oxidation is associated with Alzheimer's disease (AD), quite possibly arising from imbalances in metal ion (e.g., Fe and Cu) homeostasis.^{1c,6} Oxidative and/or nitrosative "stress" may in fact be attributed to the association of copper ion with amyloid beta (Aβ) peptides which are crucially involved in AD,⁷ as they aggregate and deposit as

Scheme 1. Transition Metal-Bound PN (⁻OOON=O) Chemistry



amyloid plaques and neurofibrillary tangles that are found between damaged neurons in AD patient's brains.⁸ The N-terminus of the Aβ peptides is a copper binding region (which includes His 6, His 13, and His 14),^{1c,6f,9} and it has lately been shown that nitration of amino acid Tyr-10 may greatly enhance Aβ aggregation.^{8c,10} A recent computational study shows that Aβ bound to Cu²⁺ ion could generate PN in the presence of ascorbate, nitric oxide, and dioxygen.¹¹ In fact, this proposal has

Received: October 12, 2016

Published: December 2, 2016

separate experimental backing, in that ligand–copper complexes have in the past few years been shown to be able to form LCu(–OON=O) species,¹² with reactions of Cu^I with O_{2(g)}^{12a} and then NO_(g) or Cu^I–NO with O_{2(g)} (Scheme 1).^{12b–e}

Bioinspired chemical systems have shown that coordination complexes with a number of different metal ions, along with sources of NO_(g) and O_{2(g)}, can lead to the generation of metal-bound PN species. Koppenol and co-workers¹³ reported the first isolated PN complex of cobalt(III), from reaction of a pentacyano-cobalt(III) superoxide compound reacting with NO_(g) to give [Co^{III}(CN)₅(–OON=O)]^{3–} (Scheme 1). Kurtikyan and co-workers¹⁴ have more recently published on porphyrinate Co^{III}–PN complexes, thoroughly characterized by infrared (IR) spectroscopy and density functional theory (DFT) calculations. A heme–superoxo complex was implicated to form from reaction of a heme–superoxo species with NO_(g), as it led to a nitrate heme-Fe^{III}(NO₃[–]) species by isomerization (Scheme 1).¹⁵ In aqueous chemistry, PN rapidly isomerizes to nitrate in ~90% yield;¹⁶ in fact, the application of this reaction to PN decomposition catalysis has been a subject of intense research.¹⁷ Such catalysts have been shown to exhibit highly favorable biological effects.^{2g,18}

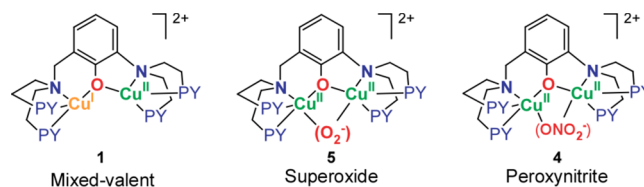
Peroxynitrite–metal complexes may also form as intermediates in the oxygenation of metal–nitrosyl complexes,¹⁹ such as first reported by Basolo,²⁰ ultimately giving nitrite products (Scheme 1). For two cases involving copper–peroxynitrite complexes,^{12a,b} LCu^{II}–PN complexes thermally transform to give LCu^{II}–nitrite products plus dioxygen. This seems to also correspond to known aqueous chemistry: peroxynitrite decomposes through various pathways,^{3c,21} including its degradation according to 2[–]OON=O → O₂ + 2NO₂[–] under basic conditions and relatively high concentrations,^{21b,d,e} and such reactivity has even been observed in aqueous chemistry with copper ion.²² Similarly, Nam and co-workers reported formation of macrocyclic ligand-bound metal–PN complexes, for example, LCr^{III}–PN²³ and non-heme-Fe^{III}–PN²⁴ species, generated from precursor M–O₂ adducts reacting with NO_(g) (Scheme 1). A novel case involves reaction of a macrocyclic ligand (L)Co–nitrosyl complex with potassium superoxide (KO₂), leading to LCo^{III}–nitrite + 1/2 O_{2(g)} products, all proceeding through putative Co–PN intermediates (Scheme 1).²⁵

Peroxynitrite heme species are also of great interest, since it is hypothesized that an intermediate heme Fe^{III}(–OON=O) species forms in NO dioxygenases; these function to maintain NO_(g) homeostasis by oxidizing excess nitric oxide present to nitrate ion.^{2g,19a,26} This may occur via reaction of NO_(g) with an oxy-heme (i.e., Fe^{III}(–O₂^{•–})) complex. The resulting PN complex is thought to then undergo O–O homolysis to generate nitrogen dioxide (•NO₂), which may either couple with the ferryl O-atom (i.e., Fe^{IV}=O) produced by the O–O homolysis to give the nitrate ion product, or couple to a nearby phenoxyl (i.e., tyrosyl) radical to give a nitrated Tyr residue. (Note, the tyrosyl radical would have formed by an internal protein ArOH substrate oxidation from a high-valent ferryl species also formed via homolysis reactions; Scheme 1, M⁽ⁿ⁺¹⁾⁺=O). Chemical studies show that such reactivity can be observed in met-myoglobin (Mb) + PN reactions.²⁷ However, complementary Mb/O₂ + NO_(g) reactions seem to not produce such intermediates.²⁸

Following the now known M–O_{2(g)} + NO_(g) biological and chemical examples to give PN and subsequent reactions, plus the likely importance of copper in chemical or biological

systems,^{1c,6,7,9,12f} we report here on a new system involving binuclear copper species, which gives rise to chemistry not previously observed, providing new insights. In the past, we performed extensive studies concerning the binucleating ligand UN–O[–],²⁹ where a phenolate O-atom bridges two copper ions. In this work, we report on the formation of a PN moiety bound to this binuclear dicopper(II) framework, [Cu^{II}₂(UN–O[–])(–OON=O)]²⁺ (4) (Chart 1).

Chart 1. Mixed-Valent Dicopper Complex [Cu^ICu^{II}(UN–O[–])]²⁺ (1), Superoxide Dicopper(II) Complex [Cu^{II}₂(UN–O[–])(O₂^{•–})]²⁺ (5), and Peroxynitrite Dicopper(II) Complex [Cu^{II}₂(UN–O[–])(–OON=O)]²⁺ (4)



Complex 4 can be generated by either of the pathways discussed: (a) Mⁿ⁺ + NO_(g) + O_{2(g)} (method 1) or (b) Mⁿ⁺ + O_{2(g)} + NO_(g) (method 2). (See also Scheme 1, but where Mⁿ⁺ is a mixed-valent Cu^ICu^{II} complex 1 and Mⁿ⁺ + O_{2(g)} gives rise to the fully characterized superoxide dicopper(II) complex [Cu^{II}₂(UN–O[–])(O₂^{•–})]²⁺ (5), $\nu(\text{O–O}) = 1120$ or 1140 cm^{-1} .^{29a}) Here, we report on a dicopper nitrosyl complex and intermediates involved in metal–peroxynitrite 4 formation, studied using low-temperature infrared (LT-IR) spectroscopy. Further, complex 4 is able to facilitate aromatic ring nitration chemistry, including an exogenously 2,4-di-*tert*-butylphenol (DTBP) substrate as a biological tyrosine substrate surrogate.

RESULTS AND DISCUSSION

The NO_(g) Adduct. We previously reported that, with this unsymmetrical binucleating ligand framework binding to two copper ions, a mixed-valent Cu^ICu^{II} complex (with localized electronic structure) can be synthesized, [Cu^ICu^{II}(UN–O[–])(DMF)]²⁺ (1, DMF = dimethylformamide, and with two SbF₆[–] non-coordinating anions), with the carbonyl O-atom in the DMF molecule binding to the Cu(II) ion in the solid state.^{29a}

Complex 1 is found to react with excess NO_(g) in dichloromethane (DCM) as solvent, at –80 °C (see Experimental Section), to form a complex that we formulate as a mixed-valent copper–nitrosyl complex, [Cu^ICu^{II}(UN–O[–])(μ–•NO)]²⁺ (2) (Figure 1a). The formation of 2 is accompanied by a change in the ultraviolet–visible (UV–vis) spectra, with the disappearance of the $\lambda_{\text{max}} = 350 \text{ nm}$ absorption of 1 and appearance of more complex features at $\lambda_{\text{max}} = 383$ and 546 nm (see Supporting Information, Figure S1).³⁰

We justify the description of the NO adduct as [Cu^ICu^{II}(UN–O[–])(μ–•NO)]²⁺ (2) on the basis of the following observations and analysis/arguments:

- Using LT-IR, we observed a new band grow in at 1670 cm^{-1} after addition of NO_(g) to the solution of complex 1 (Figure 1b). This value of 1670 cm^{-1} ($\Delta^{15}\text{NO} = -25 \text{ cm}^{-1}$, Figure S3) is comparable with the signals of many other Cu^I–NO_(g) adducts, for which $\nu(\text{N–O})$ is often observed to occur above 1700 cm^{-1} (Table 1).
- This $\nu(\text{N–O}) = 1670 \text{ cm}^{-1}$ value for 2 is considerably higher than that which was found much earlier for the

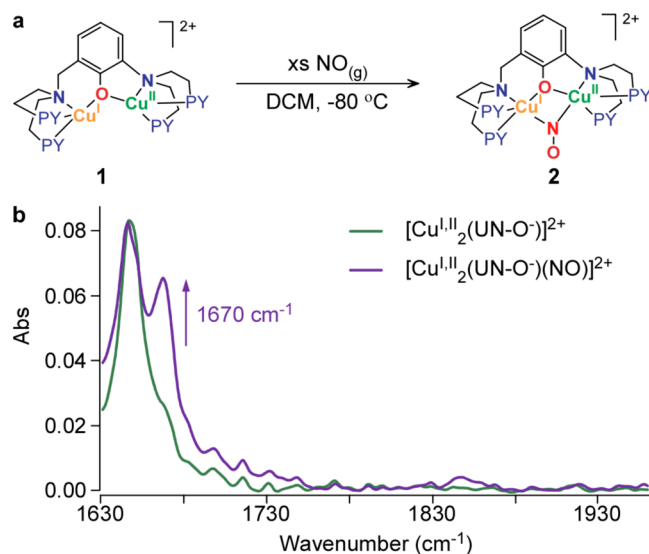


Figure 1. (a) $[\text{Cu}^{\text{I}}\text{Cu}^{\text{II}}(\text{UN-O}^-)]^{2+}$ (**1**) reacts with excess $\text{NO}_{(\text{g})}$ to form $[\text{Cu}^{\text{II}}(\text{UN-O}^-)(\text{NO})]^{2+}$ (**2**) at $-80\text{ }^\circ\text{C}$ in dichloromethane (DCM) solvent. (b) Low-temperature ($-80\text{ }^\circ\text{C}$) infrared spectroscopy of the complex **1** (green line spectrum) reacting with $\text{NO}_{(\text{g})}$ to form complex **2** (in purple). The 1670 cm^{-1} full spectrum formed within 1 min after addition of $\text{NO}_{(\text{g})}$.

Table 1. N–O Stretching Frequencies in LCu–NO Complexes^a

LCu–NO	$\nu(\text{N-O})$ ($^{15}\text{N-O}$), cm^{-1}	ref
$[\text{Cu}^{\text{II}}_2(\text{XYL-O}^-)(\text{NO}^-)]^{2+}$	1536	31
$[\text{Cu}^{\text{II}}(\text{UN-O}^-)(\text{NO})]^{2+}$	1670 (1645)	this work
$[\text{Cu}^{\text{I}}\text{HB}(3\text{-}^t\text{Bu-5-}^i\text{Prpz})_3(\text{NO})]$	1698 (1627 ^b)	32
$[\text{Cu}^{\text{I}}\text{HB}(\text{Bupz})_3(\text{NO})]$	1712 (1679)	33
$[\text{Cu}^{\text{I}}(\text{AN})(\text{NO})]^+$	1736 (1714)	12b
$[\text{Cu}^{\text{I}}\text{HC}(3\text{-}^t\text{Bu-5-}^i\text{Prpz})_3(\text{NO})]^+$	1742 (1666 ^b)	32
$[\text{Cu}^{\text{II}}(\text{L})(\text{NO})]^+$	1846 (1815)	34
$[\text{Cu}^{\text{II}}_2(\text{UN-O}^-)(\text{O}_2^-)(\text{NO})]^{2+}$	1853 (1820)	this work
$[\text{Cu}^{\text{II}}(\text{CH}_3\text{NO}_2)_5(\text{NO})]^{2+}$	1933 (1893)	35

^aSee the SI (Figure S2) for full drawings of the ligands and their IUPAC names. ^bValues for $\nu(^{15}\text{N}-^{18}\text{O})$.

closely related dicopper(II) analogue $[\text{Cu}^{\text{II}}_2(\text{XYL-O}^-)(\text{NO}^-)]^{2+}$ ($\nu(\text{N-O}) = 1536\text{ cm}^{-1}$, Table 1), with symmetrical binucleating ligand XYL-O^- , synthesized from the addition of 1 equiv of nitrosonium hexafluorophosphate (NOPF_6) to the dicopper(I) complex $[\text{Cu}^{\text{I}}_2(\text{XYL-O}^-)]^+$ at room temperature in DCM solvent (Chart 2).³¹ In $[\text{Cu}^{\text{II}}_2(\text{XYL-O}^-)(\text{NO}^-)]^{2+}$, the very low $\nu(\text{N-O})$ value and structural aspects³¹ of the complex indicate that a formal negative charge is located on the nitrosyl ligand; i.e., it is a nitroxyl-containing compound with a NO^- moiety.³¹ The considerably higher $\nu(\text{N-O})$ value in **2** is thus more consistent with what is expected for a $\text{Cu}^{\text{I}}-\text{NO}_{(\text{g})}$ adduct (Figure 1a).

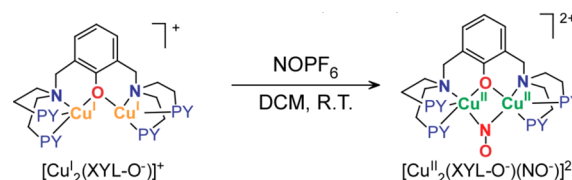
(iii) $\text{Cu}^{\text{I}}-\text{NO}_{(\text{g})}$ adducts in mononuclear cases are, in general, best described as $\text{Cu}^{\text{I}}-(^*\text{NO})$ species in terms of their electronic structures,³⁶ and electron paramagnetic resonance (EPR) spectra of such species do in fact exhibit $g \approx 2$ organic radical signals and not spectra associated with $\text{Cu}(\text{II})$, such as would be expected for a $\text{Cu}^{\text{II}}-(\text{NO}^-)$ formulation and associated electronic structure. Complex **2** is EPR silent (as confirmed

experimentally), which comes about from the fact that there is an additional $\text{Cu}(\text{II})$ ion present, as the complex is binuclear; so overall this is an even spin system (i.e., one unpaired electron on the $^*\text{NO}$ ligand and another on the $\text{Cu}(\text{II})$ ion).

(iv) Further, the lower value of $\nu(\text{N-O})$ in complex **2** compared to most other $\text{Cu}^{\text{I}}-\text{NO}_{(\text{g})}$ adducts, which have $\nu(\text{N-O}) > 1700\text{ cm}^{-1}$ (Table 1), leads us to thoughts that the NO moiety bridges through its N-atom, binding both the Cu^{I} and Cu^{II} ions in $[\text{Cu}^{\text{I}}\text{Cu}^{\text{II}}(\text{UN-O}^-)(\mu\text{-}^*\text{NO})]^{2+}$ (**2**) (Figure 1a).

(v) Another argument in favor of this supposition is that, if the nitrosyl ligand does not bind to the Cu^{II} ion, the latter would only be tetracoordinate; however, Cu^{II} ion strongly prefers pentacoordination; so, addition of this bridging nitrosyl as a fifth ligand to Cu^{II} seems reasonable.

Chart 2. Formation of Nitroxyl Complex $[\text{Cu}^{\text{II}}_2(\text{XYL-O}^-)(\text{NO}^-)]^{2+}$



In summary, complex **2**, the product of addition of $\text{NO}_{(\text{g})}$ to mixed-valent complex $[\text{Cu}^{\text{I}}\text{Cu}^{\text{II}}(\text{UN-O}^-)]^{2+}$ (**1**), is best described as a mixed-valent copper–nitrosyl complex, $[\text{Cu}^{\text{I}}\text{Cu}^{\text{II}}(\text{UN-O}^-)(\mu\text{-}^*\text{NO})]^{2+}$ (**2**) (Figure 1a).

Addition of $\text{O}_{2(\text{g})}$ to $[\text{Cu}^{\text{II}}_2(\text{UN-O}^-)(\mu\text{-}^*\text{NO})]^{2+}$ (2**).** After removal of excess $\text{NO}_{(\text{g})}$ from the solution of **2** by the application of vacuum/purge cycles (Figure 2b, spectrum in purple), bubbling the solution of **2** with $\text{O}_{2(\text{g})}$ resulted in the disappearance of the N–O stretch of 1670 cm^{-1} , while a new band at 1853 cm^{-1} grew in (Figure 2b, spectrum in red); all this was monitored utilizing *in situ* LT-IR spectroscopy. We assign this IR band at 1853 cm^{-1} ($\Delta^{15}\text{NO} = -33\text{ cm}^{-1}$, Figure S4) to the nitrosyl ligand in a new complex, **3**, now in an altered chemical environment, as discussed below. The presence of the pre-formed 1853 cm^{-1} band in the purple spectrum (Figure 2b) prior to O_2 bubbling is due to a slight air leak while applying vacuum/Ar purging. This band does not belong to **2**, as presented in Figure 1.

A literature survey of Cu–nitrosyl complexes, and even metal– $\text{NO}_{(\text{g})}$ adducts in general, suggests that this value falls into the region where the nitrosyl ligand may be best described as having a NO^+ (nitrosonium) electronic structure. A series of ligand (L)–copper(II)–nitrosyl complexes $\text{LCu}^{\text{II}}(\text{NO})$ studied by Mondal and co-workers³⁴ reveals that $\nu(\text{N-O})$ can vary between 1640 and 1846 cm^{-1} , depending on the ligand (L) environment (and thus the $\text{LCu}^{\text{II/I}}$ reduction potential). Also, Theopold and co-workers³⁷ studied a tris(3-*tert*-butyl-5-methylpyrazolyl)borate ($\text{Tp}^{t\text{-Bu,Me}}$) ligand-derived cobalt(III) superoxide complex, $\text{Tp}^{t\text{-Bu,Me}}\text{Co}^{\text{III}}(\text{O}_2^{\bullet-})$. Upon addition of $\text{NO}_{(\text{g})}$ at $-78\text{ }^\circ\text{C}$, a new band at 1849 cm^{-1} grew in and was assigned as an absorption of an unstable nitrosyl intermediate. A very interesting example from Hayton and co-workers³⁵ is a pentanitromethane-coordinated $\text{Cu}^{\text{II}}-\text{NO}$ compound, where $\nu(\text{N-O}) = 1933\text{ cm}^{-1}$. This is suggestive of a nitrosonium characterization of the nitrosyl ligand, and the compound is

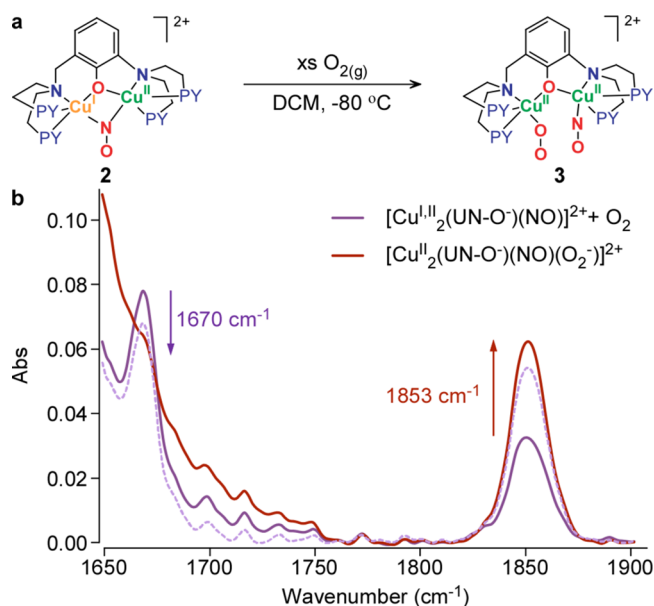


Figure 2. (a) $[\text{Cu}^{\text{II}}_2(\text{UN}-\text{O}^-)(\text{NO})]^{2+}$ (**2**) reacts with excess $\text{O}_2(\text{g})$ to form $[\text{Cu}^{\text{II}}_2(\text{UN}-\text{O}^-)(\text{NO})(\text{O}_2^-)]^{2+}$ (**3**) at -80°C in DCM. (b) Low-temperature infrared spectroscopy of the complex **2** (spectrum in purple) reacting with $\text{O}_2(\text{g})$ to form complex **3** (spectrum in red) at -80°C . The dotted purple spectrum shows the transition for the reaction mentioned above. The last spectrum in red was taken 5 min after addition of $\text{O}_2(\text{g})$.

reported to have a $[\text{Cu}^{\text{II}}(\text{CH}_3\text{NO}_2)_5(\text{NO})]^{2+}$ formulation, while the NO moiety is bound to the Cu^{II} ion in a bent fashion ($\angle\text{Cu}-\text{N}-\text{O} = 121^\circ$). Thus, addition of $\text{NO}(\text{g})$ to $\text{Cu}(\text{II})$ gives adducts described either as $\text{LCu}^{\text{II}}-(\text{NO})$ or $\text{LCu}^{\text{I}}-\text{NO}^+$ species. Therefore, $[\text{Cu}^{\text{II}}_2(\text{UN}-\text{O}^-)(\text{NO})(\text{O}_2^-)]^{2+}$ (**3**), the product of addition of O_2 to the nitrosyl complex $[\text{Cu}^{\text{II}}_2(\text{UN}-\text{O}^-)(\mu-\text{NO})]^{2+}$ (**2**), can be described to have either the $\text{LCu}^{\text{II}}-(\text{NO})$ or $\text{LCu}^{\text{I}}-\text{NO}^+$ electronic structure.

What about the fate of the $\text{O}_2(\text{g})$ that was added? As dioxygen typically binds to transition metals in their reduced state, reaction of **2** with O_2 likely involves electron transfer from the cuprous ion in **2**, leading to a cupric superoxide ($\text{O}_2^{\bullet-}$) species (thus, we place the O_2 -derived ligand on the left-hand copper ion, as represented by the drawing in Figure 2a; we cannot preclude that the diatomic ligands switch positions once **3** fully forms). To account for the changes occurring when one $\text{NO}(\text{g})$ molecule is added to **1** to give **2** with a single nitrosyl ligand (excess $\text{NO}(\text{g})$ removed by vacuum/purge cycles), followed by $\text{O}_2(\text{g})$ addition to **2** (with excess $\text{O}_2(\text{g})$ removed) giving complex **3**, we must formulate the latter as a superoxide and nitrosyl complex $[\text{Cu}^{\text{II}}_2(\text{UN}-\text{O}^-)(\text{NO})(\text{O}_2^-)]^{2+}$ (**3**) (Figure 3a).³⁸ The conclusion that this compound contains a single $\text{NO}(\text{g})$ plus a single $\text{O}_2(\text{g})$ -derived ligand, as per this formulation, is further supported by its subsequent transformation to a PN complex, $[\text{Cu}^{\text{II}}_2(\text{UN}-\text{O}^-)(-\text{OON}=\text{O})]^{2+}$ (**4**), which “logically” forms by the intramolecular coupling of the superoxide ligand with the electrophilic N-atom of the adjacent NO (or NO^+) molecule.

$[\text{Cu}^{\text{II}}_2(\text{UN}-\text{O}^-)(\text{NO})(\text{O}_2^-)]^{2+}$ (3**) Converts to the Peroxynitrite Complex $[\text{Cu}^{\text{II}}_2(\text{UN}-\text{O}^-)(-\text{OON}=\text{O})]^{2+}$ (**4**).** Using LT-IR spectroscopy, it is seen that the change from **3** to **4** occurs over the course of 20 min (-80°C), and the $\nu(\text{N}-\text{O}) = 1853\text{ cm}^{-1}$ band disappears. The formation of peroxynitrite-dicopper(II) complexes $[\text{Cu}^{\text{II}}_2(\text{UN}-\text{O}^-)(-\text{OON}=\text{O})]^{2+}$ (**4**) is

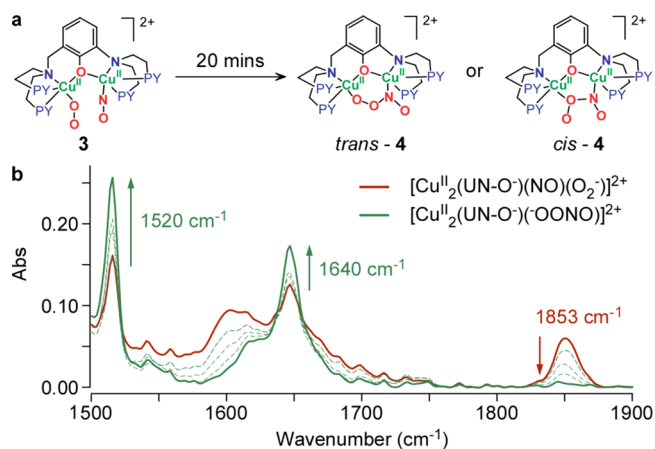


Figure 3. (a) $[\text{Cu}^{\text{II}}_2(\text{UN}-\text{O}^-)(\text{NO})(\text{O}_2^-)]^{2+}$ (**3**) gradually transforms to form the $[\text{Cu}^{\text{II}}_2(\text{UN}-\text{O}^-)(-\text{OON}=\text{O})]^{2+}$ (**4**) complex at -80°C . (b) Low-temperature infrared spectroscopy of complex **3** (red line), which changes to form complex **4** (solid green line spectrum) over the course of 20 min.

suggested by the appearance of new IR bands at 1520 cm^{-1} ($\Delta^{15}\text{NO} = -20\text{ cm}^{-1}$) and 1640 cm^{-1} ($\Delta^{15}\text{NO} = -26\text{ cm}^{-1}$),³⁰ assignable to the $\text{N}=\text{O}$ double bond of the PN ligand (Figures 3b and S7).

We assign these bands to two different species (conformers), *cis*- and *trans*-PN complexes, respectively (Figure 3a), as also discussed further below. When the N-atom on the NO moiety forms a bond with the distal (to Cu) O-atom of the dioxygen-derived moiety (i.e., the $\text{O}_2^{\bullet-}$ ligand), a *trans*-PN complex is likely formed. However, if or when the proximal superoxide O-atom attacks the electrophilic nitrosyl N-atom (*vide supra*), the *cis*-PN complex can be generated, as shown in Figure 3a.³⁹

In a different route leading to the formation of PN complex **4** (method 2, see Abstract/TOC figure), we performed a series of LT-IR experiments starting from the mixed-valent complex $[\text{Cu}^{\text{I}}_2(\text{UN}-\text{O}^-)(\text{DMF})]^{2+}$ (**1**). Addition of excess $\text{O}_2(\text{g})$ via syringe does not incur any significant IR spectral change (Figure S5), even though we know that the superoxo-dicopper(II) complex $[\text{Cu}^{\text{II}}_2(\text{UN}-\text{O}^-)(\text{O}_2^{\bullet-})]^{2+}$ (**5**) forms, as previously described.^{29a} After removal of any excess $\text{O}_2(\text{g})$ through vacuum/purge cycles, an ~ 7 -fold excess of $^{15}\text{NO}(\text{g})$ was added directly into the solution of **5** using a gastight syringe.

We then observed the formation of the same superoxide and $^{15}\text{NO}(\text{g})$ -labeled nitrosyl complex $[\text{Cu}^{\text{II}}_2(\text{UN}-\text{O}^-)(\text{NO})(\text{O}_2^{\bullet-})]^{2+}$ (**3**), with 1820 cm^{-1} IR absorption (Figure S6), which, as before, leads to the formation of PN complex $[\text{Cu}^{\text{II}}_2(\text{UN}-\text{O}^-)(-\text{OON}=\text{O})]^{2+}$ (**4**) over the course of 20 min (Figure S7).

Although IR studies on PN bound to copper ions are not available in the literature, the *cis*- and *trans*-PN N–O stretching frequencies for alkali metals are determined to be in the region of ~ 1440 and $\sim 1580\text{ cm}^{-1}$, respectively (Table 2). So, the difference in $\nu(\text{N}-\text{O})$ between the *cis*- and *trans*-PN conformers can be quite large, i.e., $>100\text{ cm}^{-1}$,⁴⁰ as is observed here for our *cis*- and *trans*-conformers of the PN complex $[\text{Cu}^{\text{II}}_2(\text{UN}-\text{O}^-)(-\text{OON}=\text{O})]^{2+}$ (**4**). We can thus assign the 1520 and 1640 cm^{-1} IR bands to the *cis*- and *trans*-conformers, respectively (Table 2).

A literature survey on IR data for a few transition metal–peroxynitrite complexes supports our assignments for $[\text{Cu}^{\text{II}}_2$

Table 2. N–O Stretching Frequency in $L_nM_x(-OON=O)$ Complexes^a

$L_nM_x(-OON=O)$	$\nu(N=O)$ cm^{-1}	ref
<i>cis</i> -NaOONO	1422	40
<i>cis</i> -KOONO	1444	40
$[\text{Cu}^{\text{II}}_2(\text{UN}-\text{O}^-)(\text{cis}^- \text{OON}=\text{O})]^{2+}$	1520	this work
<i>trans</i> -KOONO	1528	40
<i>trans</i> -NaOONO	1580	40
$[\text{Fe}(\text{TMEDA})(\text{NO})(^- \text{OON}=\text{O})]$	1589	41
$(\text{NH}_3)_3\text{Co}(\text{TTP})(^- \text{OON}=\text{O})$	1596	14
$[\text{N}(\text{CH}_2\text{CH}_3)_3][\text{Co}(\text{CN})_5(^- \text{OON}=\text{O})]$	1621	13
$[\text{Cu}^{\text{II}}_2(\text{UN}-\text{O}^-)(\text{trans}^- \text{OON}=\text{O})]^{2+}$	1640	this work

^aSee SI for drawings of the ligands and IUPAC names.

$(\text{UN}-\text{O}^-)(^- \text{OON}=\text{O})]^{2+}$ (4). With a porphyrinate¹⁴ or cyano¹³ group as co-ligand in Co(III) complexes, the $\text{O}-\text{N}=\text{O}$ $\text{N}=\text{O}$ (double-bond) IR stretching frequencies range from 1600 to ~ 1620 cm^{-1} (Table 2). Kurtikyan and co-workers¹⁴ observed $\nu(\text{N}=\text{O})$ for the PN ligand in $(\text{NH}_3)_3\text{Co}(\text{TTP})(^- \text{OON}=\text{O})$ (TTP = *meso*-tetra-*p*-tolylporphyrinato dianion) at 1596 cm^{-1} , assigned to be in a *trans* conformation and ligated axially via the peroxy nitrite anionic O-atom. Their DFT calculations supported this assignment, also giving a calculated value of $\nu(\text{N}-\text{O}) = 1678$ cm^{-1} . In another example, Kim and co-workers⁴¹ reported that, with a bidentate tetramethylethylenediamine ligand bound in an iron–dinitrosyl complex, oxygenation results in the generation of a new $\nu(\text{N}-\text{O})$ band at ~ 1590 cm^{-1} , assigned by those researchers to a *trans*-PN complex (Table 2). As noted, we assign our dicopper complex with *cis*-PN ligand, $[\text{Cu}^{\text{II}}_2(\text{UN}-\text{O}^-)(\text{cis}^- \text{OON}=\text{O})]^{2+}$ (4), as having $\nu(\text{N}-\text{O}) = 1520$ cm^{-1} , a much lower value than for these other coordination complexes.

Formation of $[\text{Cu}^{\text{II}}_2(\text{UN}-\text{O}^-)(^- \text{OON}=\text{O})]^{2+}$ (4) Followed by UV–Vis Spectroscopy. As described above, the LT-IR studies reveal that, for the PN complex 4, the mixture of conformers can be formed either by addition of O_2 to the nitrosyl complex $[\text{Cu}^{\text{I}}_2(\text{UN}-\text{O}^-)(\mu-\text{NO})]^{2+}$ (2) or by addition of $\text{NO}_{(\text{g})}$ to the superoxide complex $[\text{Cu}^{\text{II}}_2(\text{UN}-\text{O}^-)(\text{O}_2^{\bullet-})]^{2+}$ (5).^{29a}

In fact, this finding is also supported by UV–vis spectroscopic monitoring. Following the generation of 5 by addition of $\text{O}_{2(\text{g})}$ to the mixed-valent complex 1, one obtains the spectrum with $\lambda_{\text{max}} = 404$ nm (dark green solid line spectrum, Figure 4b). After removal of excess $\text{O}_{2(\text{g})}$ and addition of excess $\text{NO}_{(\text{g})}$ (~ 20 equiv) into the solution of 5 using a gastight syringe, an isosbestic conversion occurring over ~ 10 min is observed for the transformation to form the PN complex 4 with $\lambda_{\text{max}} = 355$ (sh), 420 (sh), and 680 nm (blue spectrum, Figure 4b).

The reaction of 2 with O_2 to give 3 (Figure 2a) and finally leading to 4 (Figure 3a), monitored by LT-IR spectroscopy and described above, was also monitored by UV–vis spectroscopy. This was carried out at low concentrations, ~ 100 times more dilute than for the LT-IR studies. The result is that, at the UV–vis scale, the nitrosyl–superoxo complex $[\text{Cu}^{\text{II}}_2(\text{UN}-\text{O}^-)(\text{NO})(\text{O}_2^{\bullet-})]^{2+}$ (3) is metastable; UV–vis spectral transformations on going from 2 to 4 were monitored (Figure S1), but stable UV–vis feature for 3 could not be obtained.³⁰

Low-Temperature Electrospray Ionization Mass Spectrometry (ESI-MS) of $[\text{Cu}^{\text{II}}_2(\text{UN}-\text{O}^-)(^- \text{OON}=\text{O})]^{2+}$ (4). ESI-MS was employed to further confirm the formulation for 4. Upon injection of a cold solution (-80 °C) of complex 4,

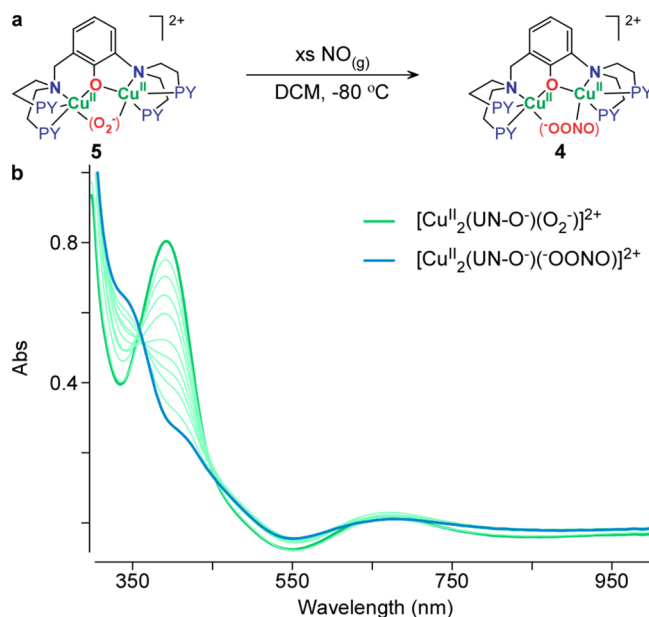


Figure 4. (a) $[\text{Cu}^{\text{II}}_2(\text{UN}-\text{O}^-)(\text{O}_2^{\bullet-})]^{2+}$ (5) reacts with excess nitric oxide gas at -80 °C to form the complex $[\text{Cu}^{\text{II}}_2(\text{UN}-\text{O}^-)(\text{O}_2\text{NO})]^{2+}$ (4). (b) UV–vis spectroscopy of the transformation from the superoxide $[\text{Cu}^{\text{II}}_2(\text{UN}-\text{O}^-)(\text{O}_2^{\bullet-})]^{2+}$ (5) to $[\text{Cu}^{\text{II}}_2(\text{UN}-\text{O}^-)(^- \text{OON}=\text{O})]^{2+}$ (4) by addition of excess nitric oxide gas at -80 °C.

prepared in a solvent mixture of 80% DCM and 20% acetonitrile (ACN), a peak for complex 4 as adduct with one SbF_6^- counteranion was observed as the monocation complex $[\text{Cu}^{\text{II}}_2(\text{UN}-\text{O}^-)(^- \text{OON}=\text{O})]^{2+}(\text{SbF}_6^-)$, i.e., a peak at $m/z = 981.92$ for complex 4 prepared with $^{16}\text{O}_{2(\text{g})}$. When superoxide complex 5 was prepared using $^{18}\text{O}_{2(\text{g})}$, the m/z value changed to 986.02 (Figure 5). These values are in very good agreement with the theoretically predicted values of 982.04 for complex 4 with $^{16}\text{O}_{2(\text{g})}$ and 986.05 for complex 4 with $^{18}\text{O}_{2(\text{g})}$.

Phenol Nitration by Complex $[\text{Cu}^{\text{II}}_2(\text{UN}-\text{O}^-)(^- \text{OON}=\text{O})]^{2+}$ (4). As described in the Introduction, peroxy nitrite, or even metal-mediated peroxy nitrite reactions are most likely responsible for biological tyrosine phenol side-chain or *in vitro* phenol substrate nitration, often biologically damaging. Beckman^{2b,c,g} and Koppenol^{2c} have discussed this in particular for the interaction of PN with the enzyme CuZn-superoxide dismutase or Fe^{III} -EDTA (or other) coordination complexes and postulate that metal ions favor heterolytic cleavage of the PN O–O bond to give nitronium ion (NO_2^+), which is a powerful nitrating agent. More recently, Girault^{12f} has shown that copper ion complexes may mediate PN formation and then phenol nitration. Metal-bound PN complexes have now been shown by other groups^{12a,c,e,f,41} to react with substituted phenols, in particular 2,4-di-*tert*-butylphenol (DTBP) as an analytically useful substrate.

Thus, it was of considerable interest to examine the behavior of 4 with DTBP. Upon addition of 1 equiv of this substrate to the superoxide–dicopper(II) complex $[\text{Cu}^{\text{II}}_2(\text{UN}-\text{O}^-)(\text{O}_2^{\bullet-})]^{2+}$ (5) formed in DCM at -80 °C (green spectrum in Figure 6b), there was no apparent change. The PN complex $[\text{Cu}^{\text{II}}_2(\text{UN}-\text{O}^-)(^- \text{OON}=\text{O})]^{2+}$ (4) was then generated *in situ* by first removing excess dioxygen and then adding $\text{NO}_{(\text{g})}$ (blue spectrum), followed by removing any excess *in vacuo*. This results in an immediate reaction (by this benchtop UV–vis monitoring) and the formation of a new species, identified as the previously well-known^{29a} μ -OH complex $[\text{Cu}^{\text{II}}_2(\text{UN}-$

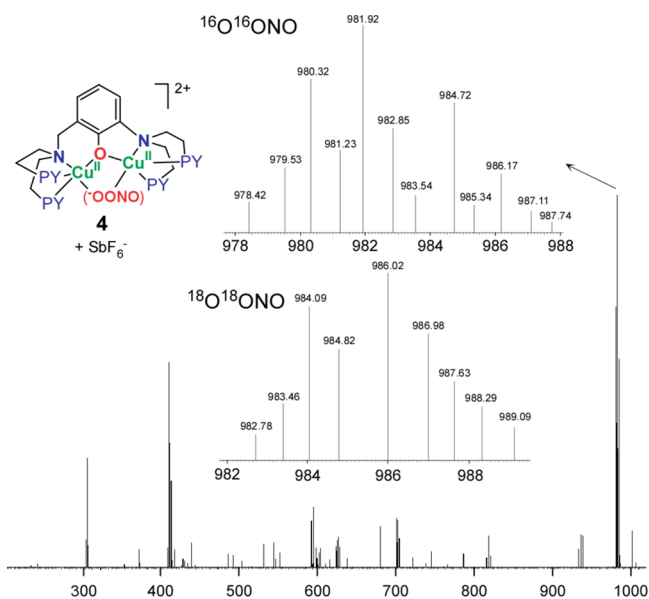


Figure 5. Low-temperature ESI-MS spectrum of the peroxynitrite complex $[\text{Cu}^{\text{II}}_2(\text{UN-O}^-)(-\text{OONO})]^{2+}$ (**4**) as adduct with one SbF_6^- anion, to give an overall detected monocation. Expanded spectra are shown above the full spectrum corresponding to m/z (greatest intensity peak) = 981.92 and that where $^{18}\text{O}_2$ was employed in the synthesis, m/z = 986.02. Good agreement is also observed for comparison of the distribution of peaks due to the presence of different isotopes (mainly due to ^{63}Cu and ^{65}Cu), experiment vs theory; see the SI.³⁰

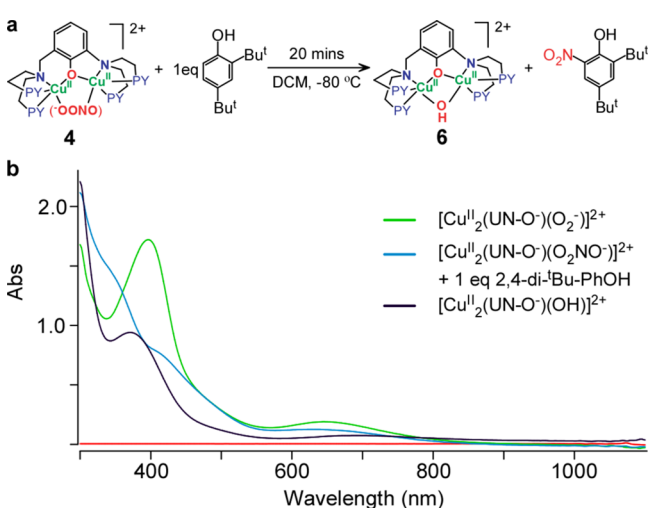


Figure 6. UV-vis spectroscopy of the formation of the superoxide $[\text{Cu}^{\text{II}}_2(\text{UN-O}^-)(\text{O}_2^{\cdot-})]^{2+}$ (**5**) (green spectrum) and the generation of the peroxynitrite complex $[\text{Cu}^{\text{II}}_2(\text{UN-O}^-)(-\text{OONO})]^{2+}$ (**4**) (blue spectrum) and the final product of $[\text{Cu}^{\text{II}}_2(\text{UN-O}^-)(\text{OH})]^{2+}$ (**6**) (black spectrum) by reacting with DTBP at -80°C in DCM.

$\text{O}^-)(\text{OH})]^{2+}$ (**6**, $\lambda_{\text{max}} = 348$ nm, black spectrum, Figure 6b), formed nearly quantitatively based on known absorptivity data. Warming of this solution to room temperature, followed by workup and analysis of the reaction mixture using gas chromatography-mass spectrometry (GC-MS; see the SI), showed that 2,4-di-*tert*-butyl-6-nitrophenol formed, essentially in 100% yield (Figure S11).³⁰ Thus, the reaction which has occurred is the stoichiometric reaction shown in Figure 6a.

In accordance with the above discussions, we suggest that the PN complex $[\text{Cu}^{\text{II}}_2(\text{UN-O}^-)(-\text{OON}=\text{O})]^{2+}$ (**4**) has under-

gone O–O bond heterolytic cleavage to produce the nitronium (NO_2^+) ion, which efficiently nitrates the DTBP substrate, this being standard electrophilic aromatic substitution chemistry. The dicopper complex initially formed upon O–O cleavage would be an oxo (oxide, O^{2-})-bridged dicopper(II) complex, $[\text{Cu}^{\text{II}}_2(\text{UN-O}^-)(\text{O}^{2-})]^{2+}$ (**7**), where the dianionic oxide ligand is stabilized by the two Cu(II) ions present. In fact, we previously isolated the oxo-dicopper(II) complex with the closely analogous binucleating ligand, XYL-O^- , i.e., $[\text{Cu}^{\text{II}}_2(\text{XYL-O}^-)(\text{O}^{2-})]^{2+}$,⁴² thus supporting our proposal. The proton released from DTBP upon its *o*-phenol nitration with NO_2^+ would then add to the highly basic oxo-atom in **7**, giving the observed μ -hydroxide complex $[\text{Cu}^{\text{II}}_2(\text{UN-O}^-)(\text{OH})]^{2+}$ (**6**) (Figure 6b). Scheme 2 outlines the reaction sequence discussed here, involving O–O heterolytic cleavage in **4**.

The reactivity, products, and product yields observed were the same when the experiment was carried out by first fully forming $[\text{Cu}^{\text{II}}_2(\text{UN-O}^-)(-\text{OON}=\text{O})]^{2+}$ (**4**), having removed excess gases, and then adding 1 equiv of DTBP. Separately, an interesting transformation occurs when **4** is warmed to room temperature in the absence of DTBP. The dicopper complex product formed is that with a *para*-nitrated central aryl-phenol within the UN-O^- ligand framework, obtained in $\sim 90\%$ yield (complex **8**, Scheme 2). The product possesses a μ -chloride bridge instead of hydroxide. The *p*-nitro group and μ -Cl atom in **8** were confirmed by X-ray diffraction analysis of this new product; the structure was reported in a recent paper.^{29a} The high yield of the product with a nitrated phenol moiety again suggests that a peroxynitrite O–O heterolytic cleavage reaction occurred, as described above, releasing NO_2^+ , which either effects nitration at the other end of the same molecule or diffuses further to nitrate a nearby dicopper complex. The μ -oxide intermediate likely formed following O–O cleavage molecule would react as a nucleophile with DCM, leading to formation of the chloride-bridged product observed. Further investigations concerning how the chloride product formed from reactions with solvent were not pursued.

Solvent Effect on the O–O Cleavage Reaction for $[\text{Cu}^{\text{II}}_2(\text{UN-O}^-)(-\text{OON}=\text{O})]^{2+}$ (4**).** In exploring further aspects of the chemistry of PN complex **4**, we happened to also perform UV-vis studies at -80°C in 2-methyltetrahydrofuran (MeTHF) as solvent. Formation of the superoxide complex $[\text{Cu}^{\text{II}}_2(\text{UN-O}^-)(\text{O}_2^{\cdot-})]^{2+}$ (**5**) in MeTHF, followed by addition of $\text{NO}_{(\text{g})}$, did lead to the rapid formation of $[\text{Cu}^{\text{II}}_2(\text{UN-O}^-)(-\text{OON}=\text{O})]^{2+}$ (**4**), as judged by the UV-vis changes observed (Figure 7). However, unlike in DCM as solvent, $[\text{Cu}^{\text{II}}_2(\text{UN-O}^-)(-\text{OON}=\text{O})]^{2+}$ (**4**) is not stable in MeTHF. In ~ 15 min (still at -80°C) the absorptivity in the 300–400 nm region starts to diminish, and eventually (after ~ 1 h) sharp peaks (spikes) grow in (Figure 7). These new absorptions are characteristic of the presence of dissolved nitrite (or actually nitrous acid, HONO);⁴³ we can conclude that HONO derives from release of $^*\text{NO}_2(\text{g})$ when **4** decomposes via homolytic O–O cleavage, *vide infra*. Nitrogen dioxide is known to attack ethers (i.e., MeTHF), effecting H-atom abstraction with the resulting formation of HONO.⁴⁴ (Note: in independent experiments we carried out, addition of $\text{NO}_2(\text{g})$ to a cold MeTHF solution slowly led to the characteristic sharp 350–400 nm absorption features, Figure S9.)

The reaction was repeated but with 1 equiv of DTBP added to the -80°C solution immediately following formation of PN complex **4**. After warming and workup of the decomposed solution, GC-MS analysis revealed that a mixture of $\sim 20\%$ bis-

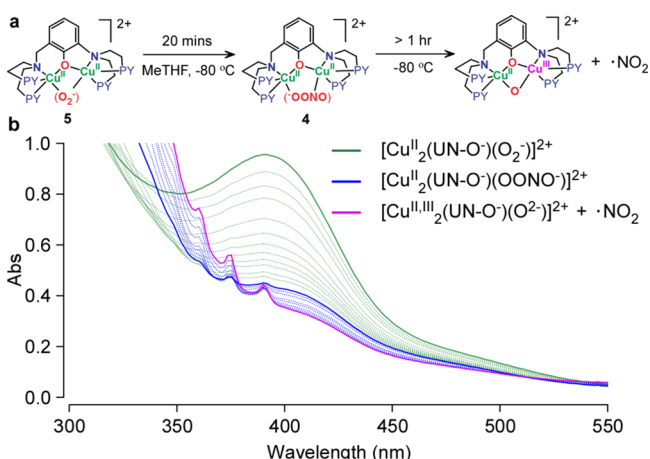
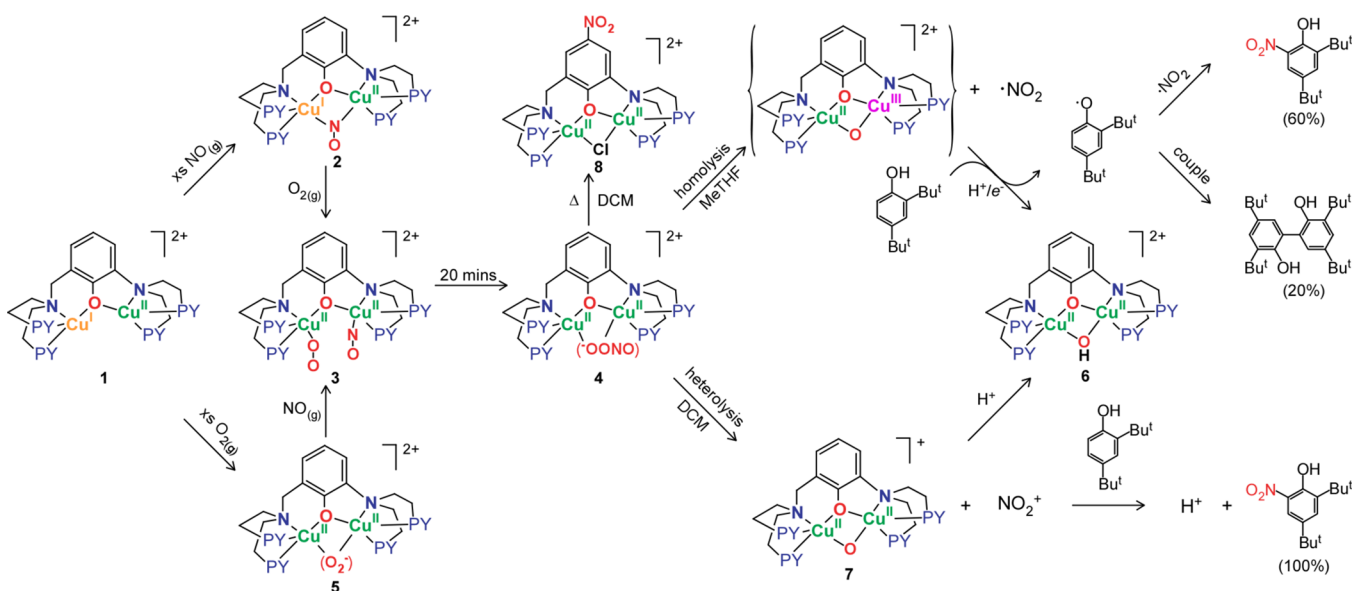
Scheme 2. PN Complex 4 Chemistry Performed at $-80\text{ }^{\circ}\text{C}$ in Solvents Dichloromethane (DCM) and 2-Methyltetrahydrofuran (MeTHF)

Figure 7. (a) Superoxide dicopper(II) complex $[\text{Cu}^{\text{II}}_2(\text{UN-O}^-)(\text{O}_2^-)]^{2+}$ (5) reacts with excess NO(g) at $-80\text{ }^{\circ}\text{C}$ in MeTHF solvent. (b) UV-vis spectroscopy of the formation and decomposition of the peroxynitrite complex $[\text{Cu}^{\text{II}}_2(\text{UN-O}^-)(\text{OONO})]^{2+}$ (4) in MeTHF to give $\cdot\text{NO}_2$ dissolved nitrogen dioxide.

phenol dimer (i.e., $\sim 40\%$ phenoxy radical coupling) and $\sim 60\%$ of the *ortho*-nitrated phenol (Scheme 2) was obtained (Scheme 2 and Figures S12–S14).

These results/observations led us to propose that, in MeTHF solvent, in contrast to the reaction in DCM, PN complex $[\text{Cu}^{\text{II}}_2(\text{UN-O}^-)(\text{OONO})]^{2+}$ (4) undergoes a homolytic O–O bond cleavage reaction. This supposition can explain the formation of a substantial quantity of bis-phenol dimer, known to be the product obtained when the phenoxy radical derived from DTBP forms. We propose that, when O–O homolytic cleavage occurs in MeTHF, $\cdot\text{NO}_2$ is formed (as observed), and the dicopper product obtained would then be formally a mixed-valent complex, $[\text{Cu}^{\text{II,III}}_2(\text{UN-O}^-)(\text{O}_2^-)]^{2+}$. This presumed transient species would be an effective H-atom abstractor, converting DTBP to its phenoxy radical derivative, which would then couple with the $\cdot\text{NO}_2$ produced to give nitrated phenol.

This is equivalent to what is proposed for many systems, including hemes, where the M^{n+} –PN species cleaves homolytically to give a $\text{M}^{n+1}=\text{O}$ complex + $\cdot\text{NO}_2$. An ArO–H substrate H-atom abstraction by $\text{M}^{n+1}=\text{O}$ and coupling to $\cdot\text{NO}_2$ leads to nitrated phenol product. However, since a phenoxy radical, ArO^\bullet , is formed during the process, some of it will self-couple, giving the bis-phenol dimer observed. Such a product cannot be explained by formation of nitronium ion obtained from heterolytic O–O peroxynitrite cleavage. Note that H-atom abstraction by a putative $[\text{Cu}^{\text{II,III}}_2(\text{UN-O}^-)(\text{O}_2^-)]^{2+}$ species would directly produce the very stable μ -hydroxide complex $[\text{Cu}^{\text{II}}_2(\text{UN-O}^-)(\text{OH})]^{2+}$,^{29a,45} that being the product identified in this reaction in MeTHF solvent. See Scheme 2 for a summary of these reactions involving PN–dicopper(II) complex heterolytic vs homolytic O–O cleavage. The solvent effect may simply be derived from the difference in dielectric constant (ϵ) of the solvents, DCM vs MeTHF, the latter being much less polar and with a smaller ϵ value. Heterolytic cleavage, producing a nitronium cation and oxide anion (although dicopper-coordinated), might be expected to be a more favorable O–O cleavage pathway in a higher dielectric solvent, and this is what is found, as described above.

CONCLUSIONS

Scheme 2 summarizes all of the chemistry observed of the UN-O^- ligand–dicopper complexes with O_2 and NO(g) chemistry. We have described the generation of a peroxynitrite complex, $[\text{Cu}^{\text{II}}_2(\text{UN-O}^-)(\text{OONO})]^{2+}$ (4), that can be formed via two pathways: (i) The mixed-valent complex $[\text{Cu}^{\text{II,III}}_2(\text{UN-O}^-)(\text{DMF})]^{2+}$ (1), when reacted with nitric oxide, forms a nitrosyl complex best described as a mixed-valent μ - $\cdot\text{NO}$ species, $[\text{Cu}^{\text{II,III}}(\text{UN-O}^-)(\text{NO})]^{2+}$ (2), which is found to form a new superoxide and nitrosyl complex, $[\text{Cu}^{\text{II}}_2(\text{UN-O}^-)(\text{NO})(\text{O}_2^-)]^{2+}$ (3), when exposed to dioxygen. However, 3 undergoes a relatively fast intramolecular coupling reaction of superoxide and nitrosyl ligands to form the peroxynitrite–dicopper(II) product 4. (ii) The superoxide adduct $[\text{Cu}^{\text{II}}_2(\text{UN-O}^-)(\text{O}_2^-)]^{2+}$ (5), reported previously to form by oxygenation of the mixed-valent complex 1, undergoes further reaction with

nitric oxide gas, producing the same new intermediate species $[\text{Cu}^{\text{II}}_2(\text{UN-O}^-)(\text{NO})(\text{O}_2^-)]^{2+}$ (3), which again transforms into the peroxyxynitrite complex $[\text{Cu}^{\text{II}}_2(\text{UN-O}^-)(\text{-OON=O})]^{2+}$ (4). The peroxyxynitrite complex 4, as deduced by IR spectroscopy, is a mixture of *cis*- and *trans*-PN forms. In any case, 4, as formed by either pathway very efficiently (even at $-80\text{ }^\circ\text{C}$), effects phenol *o*-nitration of DTBP, even with only 1 equiv of this substrate added. Our studies reveal that decomposition, or rather transformation, of the peroxyxynitrite complex 4 can proceed by heterolytic PN O–O cleavage, which putatively produces the nitronium ion (NO_2^+); in a different solvent (i.e., MeTHF), strong evidence for substantial homolytic cleavage chemistry is seen.

Thus, the major advances from this present work can be summarized as follows:

1. We report for the first time in literature that both pathways ($\text{M}^{n+} + \text{NO}_{(\text{g})} + \text{O}_{2(\text{g})}$ and $\text{M}^{n+} + \text{O}_{2(\text{g})} + \text{NO}_{(\text{g})}$) could occur in our binuclear ligand copper framework, leading to the formation of the same PN complex, $\text{M}^{(n+1)+}(\text{-OON=O})$.
2. In this synthetically challenging and biologically relevant binuclear ligand copper framework, detailed LT-IR characterizations of the key complexes are presented, and a new nitrosyl–superoxide intermediate complex $\text{M}^{(n+1)+}(\text{NO})(\text{O}_2^{\bullet-})$ is proposed to form. The intermediate transforms to the PN complex $\text{M}^{(n+1)+}(\text{-OON=O})$ that consists of both *cis*- and *trans*-conformers based on LT-IR spectroscopy.
3. In further support of the formation of PN complex $[\text{Cu}^{\text{II}}_2(\text{UN-O}^-)(\text{-OON=O})]^{2+}$ (4), it is observed to efficiently effect phenol substrate nitration.
4. Unique insights concerning the rich chemistry a metal-bound peroxyxynitrite moiety can undergo come from the observation that either O–O homolytic or heterolytic cleavage may occur. In DCM, the O–O cleavage is heterolytic, and quantitative *o*-phenol (DTBP) nitration can be attributed to the generation of nitronium ion (NO_2^+) in solution. This supposition is also supported by the observation of the efficient nitration of the ligand in the dicopper complex when in the absence of substrate DTBP. However, in the much less polar solvent MeTHF, the O–O bond undergoes homolysis to generate $\bullet\text{NO}_2$ (detected spectrophotometrically, indirectly) and a putative higher-valent complex $\text{Cu}^{\text{II,III}}_2(\text{UN-O}^-)(\text{O}_2^-)]^{2+}$ that abstracts a H-atom from DTBP to give $\text{Cu}^{\text{II}}_2(\text{UN-O}^-)(\text{OH})]^{2+}$ (as observed) and a phenoxyl radical; the latter may dimerize to form the bis-phenol observed experimentally or couple with the $\bullet\text{NO}_2$ present, leading to the observed *o*-nitrophenol.

As previously postulated,^{12a,b,f} and as supported by the rich chemistry observed here, it seems likely that copper ion chemistry with O_2 and/or NO may be important biologically, contributing significantly to (i) the known formation of nitrated protein residues (e.g., tyrosine),^{2d,f,h-1} (ii) other oxidative or nitrative damage, or (iii) possibly even signaling. In fact, peroxyxynitrite chemistry at heme centers, produced via metal/ $\text{NO}_{(\text{g})}/\text{O}_{2(\text{g})}$ chemistry, can lead to protein residue nitration. Most recently,⁴⁶ such biochemistry has been applied in the practical organic synthesis of nitrated substrates, in heme or non-heme iron enzymes.⁴⁷ The extensive chemistry observed here calls for the further investigations of the scope and mechanisms involved in metal ion-mediated peroxyxynitrite

formation and reactivity; such will, at least in part, be included in research goals in our own laboratories.

EXPERIMENTAL SECTION

Materials and Instrumentation. All chemicals were purchased from Sigma-Aldrich Co. in the highest available quality unless otherwise specified. Preparation and handling of air-sensitive compounds were achieved either using standard Schlenk line techniques under an argon atmosphere or in an MBraun Labmaster 130 nitrogen atmosphere glovebox with $\text{O}_{2(\text{g})}$ and $\text{H}_2\text{O}_{(\text{g})}$ levels <1 ppm. HPLC-grade dichloromethane (DCM), acetonitrile (ACN), and diethyl ether (Et_2O) were passed through a 60 cm long column of activated alumina under an argon atmosphere before use (Innovative Technologies, Inc.). 2-Methyltetrahydrofuran (MeTHF) was distilled over sodium benzophenone under an argon atmosphere prior to use. Solvent deoxygenation was achieved by bubbling argon through the solvent for 30 min in an addition funnel connected to a receiving Schlenk flask. Deoxygenated solvents were stored in the glovebox inside amber glass bottles and further dried over activated 3 or 4 Å molecular sieves. Dioxygen was dried by passing the gas through a short column of Drierite prior to usage. Nitric oxide was purchased from Matheson Gases and purified according to a literature method.^{15a} UV–vis absorption spectra were recorded on a Cary-50 Bio spectrophotometer using 10 mm path length Schlenk quartz cuvettes. The reaction temperature was maintained by a UnispeKs CoolSpeK cryostat controller and a cell holder kit by Unisoku Scientific Instruments. EPR samples were prepared in 5 mm o.d. quartz sample tubes (Wilmaad-LabGlass) and spectra recorded on an X-band Bruker EMX-plus spectrophotometer equipped with a dual-mode cavity (ER 4116DM) Bruker EMX CW EPR controller with a Bruker ER 041 XG microwave bridge operating at the X band ($\sim 9\text{ GHz}$). LT-IR spectra were collected on a Bruker TENSOR 27 FT-IR spectrophotometer equipped with a liquid nitrogen-chilled LN-MCT midrange detector using a Remspec 619 single-crystal sapphire fiber probe ($1100\text{--}4000\text{ cm}^{-1}$). Samples were analyzed in a custom-made Schlenk tube with two side arms and an airtight joint from which the optical probe is inserted. In a typical IR experiment, samples were first prepared in the glovebox and then transferred to the reaction tube using a 5 mL Hamilton gastight syringe. ESI-MS experiments were performed on a Thermo Finnigan LCQ Deca XP Plus spectrometer. GC-MS analysis was carried out on a Shimadzu GC-17A/GCMS0QP5050 gas chromatograph/mass spectrometer. Synthesis and characterization of the mixed-valent complex $[\text{Cu}^{\text{II,III}}_2(\text{UN-O}^-)(\text{DMF})](\text{SbF}_6)_2$, $M_w = 1229.6$, followed previously published procedures.^{29a}

Low-Temperature Infrared (LT-IR) Spectroscopy Characterization. Preparation of LT-IR samples of mixed-valent complex $[\text{Cu}^{\text{II,III}}_2(\text{UN-O}^-)(\text{DMF})](\text{SbF}_6)_2$ was conducted as follows. First, 36.8 mg (0.03 mmol) of $[\text{Cu}^{\text{II,III}}_2(\text{UN-O}^-)(\text{DMF})](\text{SbF}_6)_2$ as a brownish green crystalline solid was added to 3 mL of DCM in the glovebox. Next, 43.1 mg (0.06 mmol) of potassium tetrakis(pentafluorophenyl)borate (KBArF , $M_w = 718.3$) was added to the mixture to help fully dissolve the solid compound through anion exchange. The DCM solution was filtered, and the resulting clear solution was transferred to a 5 mL Hamilton gastight syringe. The LT-IR optical probe was placed inside a custom-made reaction tube equipped with two side arms and an airtight joint from which the optical probe is inserted. One of the arms was connected to the Schlenk line and controlled by a glass stopcock, while the other arm was sealed with a rubber septum. An inert atmosphere was established by five successive vacuum and argon purge cycles. Through the rubber septum, 3 mL of $[\text{Cu}^{\text{II,III}}_2(\text{UN-O}^-)(\text{DMF})](\text{SbF}_6)_2$ solution was added via syringe to the reaction tube, and the probe was submerged under the added solution. The tube was then placed in a dry ice/acetone bath to maintain the temperature at $-80\text{ }^\circ\text{C}$. After waiting 10 min for the temperature to equilibrate, the LT-IR spectrum for the $[\text{Cu}^{\text{II,III}}_2(\text{UN-O}^-)(\text{DMF})](\text{SbF}_6)_2$ solution was recorded over 20 scans ($1100\text{--}4000\text{ cm}^{-1}$) using the OPUS software interface.

Formation of $[\text{Cu}^{\text{II,III}}_2(\text{UN-O}^-)(\mu\text{-NO})](\text{SbF}_6)_2$. Purified nitric oxide gas, $\text{NO}_{(\text{g})}$, was collected in a 250 mL round-bottom flask and secured

with a clamp inside a fume hood. The pressure of the flask was adjusted to approximately 1 atm using a gas bubbler. A 10 mL Hamilton gastight syringe equipped with a three-way high pressure stopcock, containing a stainless steel Luer fitting attached to a Schlenk line, and 12 in. stainless steel needle was prepared. The syringe was evacuated and purged with argon gas five times, before the needle was inserted into the flask containing the purified $\text{NO}_{(\text{g})}$, and 5 mL of $\text{NO}_{(\text{g})}$ (about 7 equiv) was withdrawn. $\text{NO}_{(\text{g})}$ was gradually added to the solution of $[\text{Cu}^{\text{III}}_2(\text{UN-O}^-)(\text{DMF})](\text{SbF}_6)_2$ by puncturing the septa on the side arm of the reaction tube with the three-way syringe. The solution “trapped” in the window of the optical probe does not mix very well with the bulk solution in the reaction tube; therefore, the solution was “manually” mixed using the gastight syringe to withdraw and then quickly inject solution back into the reaction tube to achieve better mixing. The solution was then left to equilibrate at $-80\text{ }^\circ\text{C}$ for a few additional minutes, after which the LT-IR spectrum of $[\text{Cu}^{\text{III}}_2(\text{UN-O}^-)(\mu\text{-}\cdot\text{NO})](\text{SbF}_6)_2$ was monitored and recorded.

Formation of $[\text{Cu}^{\text{III}}_2(\text{UN-O}^-)(\mu\text{-}\cdot\text{NO})(\text{O}_2^{\cdot-})](\text{SbF}_6)_2$ (Method 1). $[\text{Cu}^{\text{III}}_2(\text{UN-O}^-)(\mu\text{-}\cdot\text{NO})](\text{SbF}_6)_2$ solution was put under vacuum and subsequently and purged with argon gas. This process was repeated five times to remove excess $\text{NO}_{(\text{g})}$ in the solution. A 10 mL Hamilton gastight syringe was equipped with a three-way high pressure stopcock, containing a stainless steel Luer fitting attached via rubber tubing directly to the regulator of dioxygen gas tank, and 12 in. stainless steel needle was prepared. The syringe was evacuated and purged with dioxygen gas. About 5 mL of $\text{O}_{2(\text{g})}$ was injected, through the septum sealed side arm of the reaction tube, into the solution of $[\text{Cu}^{\text{III}}_2(\text{UN-O}^-)(\mu\text{-}\cdot\text{NO})](\text{SbF}_6)_2$ and over the course of 5 min, the intermediate $[\text{Cu}^{\text{III}}_2(\text{UN-O}^-)(\mu\text{-}\cdot\text{NO})(\text{O}_2^{\cdot-})](\text{SbF}_6)_2$ was formed and IR spectrum was recorded at $-80\text{ }^\circ\text{C}$.

Formation of $[\text{Cu}^{\text{III}}_2(\text{UN-O}^-)(\text{O}_2^{\cdot-})](\text{SbF}_6)_2$ (Method 1). The solution of $[\text{Cu}^{\text{III}}_2(\text{UN-O}^-)(\mu\text{-}\cdot\text{NO})(\text{O}_2^{\cdot-})](\text{SbF}_6)_2$ was mixed several times using a gastight syringe, *vide supra*. Over the course of 20 min at $-80\text{ }^\circ\text{C}$, the LT-IR spectral features of $[\text{Cu}^{\text{III}}_2(\text{UN-O}^-)(\mu\text{-}\cdot\text{NO})(\text{O}_2^{\cdot-})](\text{SbF}_6)_2$ decreased, and new features corresponding to $[\text{Cu}^{\text{III}}_2(\text{UN-O}^-)(\text{O}_2^{\cdot-})](\text{SbF}_6)_2$ grew in.

Formation of $[\text{Cu}^{\text{III}}_2(\text{UN-O}^-)(\text{O}_2^{\cdot-})](\text{SbF}_6)_2$. First, 36.8 mg (0.03 mmol) of $[\text{Cu}^{\text{III}}_2(\text{UN-O}^-)(\text{DMF})](\text{SbF}_6)_2$ as a crystalline solid was dissolved in 3 mL of DCM, and anion exchange was performed *vide supra*. Next, 5 mL of $\text{O}_{2(\text{g})}$ was added using a three-way syringe into the solution of $[\text{Cu}^{\text{III}}_2(\text{UN-O}^-)(\text{DMF})](\text{SbF}_6)_2$ and mixed using a gastight syringe, *vide supra*. The solution was left to equilibrate for 10 min, and a spectrum was recorded at $-80\text{ }^\circ\text{C}$. The $[\text{Cu}^{\text{III}}_2(\text{UN-O}^-)(\text{O}_2^{\cdot-})](\text{SbF}_6)_2$ solution was put under vacuum and purged with argon gas. This process was repeated five times to remove excess $\text{O}_{2(\text{g})}$ in the solution.

Formation of $[\text{Cu}^{\text{III}}_2(\text{UN-O}^-)(\mu\text{-}\cdot\text{NO})(\text{O}_2^{\cdot-})](\text{SbF}_6)_2$ (Method 2). First, 5 mL of $\text{NO}_{(\text{g})}$ was added in solution of $[\text{Cu}^{\text{III}}_2(\text{UN-O}^-)(\text{O}_2^{\cdot-})](\text{SbF}_6)_2$ using a gastight syringe, *vide supra*. Over the course of 5 min, $[\text{Cu}^{\text{III}}_2(\text{UN-O}^-)(\mu\text{-}\cdot\text{NO})(\text{O}_2^{\cdot-})](\text{SbF}_6)_2$ was formed, and the LT-IR spectrum was recorded at $-80\text{ }^\circ\text{C}$.

Formation of $[\text{Cu}^{\text{III}}_2(\text{UN-O}^-)(\text{OON=O})](\text{SbF}_6)_2$ (Method 2). The solution of $[\text{Cu}^{\text{III}}_2(\text{UN-O}^-)(\mu\text{-}\cdot\text{NO})(\text{O}_2^{\cdot-})](\text{SbF}_6)_2$ was mixed several times using a gastight syringe, *vide supra*. Over the course of 20 min at $-80\text{ }^\circ\text{C}$, the LT-IR spectral features of $[\text{Cu}^{\text{III}}_2(\text{UN-O}^-)(\mu\text{-}\cdot\text{NO})(\text{O}_2^{\cdot-})](\text{SbF}_6)_2$ decreased, and new features corresponding to $[\text{Cu}^{\text{III}}_2(\text{UN-O}^-)(\text{OON=O})](\text{SbF}_6)_2$ grew in.

$^{13}\text{NO}_{(\text{g})}$ isotope-labeled LT-IR experiments were carried out in the same fashion as with $^{14}\text{NO}_{(\text{g})}$, *vide supra*. Spectra for each complex were recorded, respectively.

UV-Vis Characterization of Each Complex. **Formation of Superoxide $[\text{Cu}^{\text{III}}_2(\text{UN-O}^-)(\text{O}_2^{\cdot-})](\text{SbF}_6)_2$ by Reaction of $[\text{Cu}^{\text{III}}_2(\text{UN-O}^-)(\text{DMF})](\text{SbF}_6)_2$ with Excess $\text{O}_{2(\text{g})}$.** This spectrum was previously published.^{29a} In the reaction, 1.1 mg (0.0009 mmol) of $[\text{Cu}^{\text{III}}_2(\text{UN-O}^-)(\text{DMF})](\text{SbF}_6)_2$ as a green-color crystalline solid was dissolved in 6 mL of DCM in the glovebox to give 6 mL of 0.15 mM stock solution. Next, 3 mL of the stock solution was transferred to a custom-made 1 cm path length Schlenk cuvette, which was sealed with a rubber septum before being removed from the glovebox. The cuvette was placed inside the cell holder of the cryostat and cooled to $-80\text{ }^\circ\text{C}$.

The cuvette was left to equilibrate at $-80\text{ }^\circ\text{C}$ for 10 min, after which excess $\text{O}_{2(\text{g})}$ was added to give a green spectrum corresponding to $[\text{Cu}^{\text{III}}_2(\text{UN-O}^-)(\text{O}_2^{\cdot-})](\text{SbF}_6)_2$ in Figure 4b, *vide supra*.

UV-Vis Spectrum of $[\text{Cu}^{\text{III}}_2(\text{UN-O}^-)(\text{OON=O})](\text{SbF}_6)_2$. The solution containing $[\text{Cu}^{\text{III}}_2(\text{UN-O}^-)(\text{O}_2^{\cdot-})](\text{SbF}_6)_2$ was put under vacuum and purged with argon gas five times to remove excess $\text{O}_{2(\text{g})}$. Next, 0.2 mL of $\text{NO}_{(\text{g})}$ (about 20 equiv) was gradually added to the solution using a three-way gastight syringe, and UV-vis spectra changes were followed.

UV-Vis Spectrum of $[\text{Cu}^{\text{III}}_2(\text{UN-O}^-)(\mu\text{-}\cdot\text{NO})](\text{SbF}_6)_2$. The remaining 3 mL of the $[\text{Cu}^{\text{III}}_2(\text{UN-O}^-)(\text{DMF})](\text{SbF}_6)_2$ stock solution was transferred to a second 1 cm path length Schlenk cuvette, which was sealed with a rubber septum before being removed from the glovebox. The cuvette was placed inside the cell holder of the cryostat and cooled to $-80\text{ }^\circ\text{C}$. The cuvette was left to equilibrate at $-80\text{ }^\circ\text{C}$ for 10 min, and then 0.2 mL of $\text{NO}_{(\text{g})}$ (about 20 equiv) was added to the solution, *vide supra*, and the UV-vis spectrum was recorded.

UV-Vis Spectrum of $[\text{Cu}^{\text{III}}_2(\text{UN-O}^-)(\text{OON=O})](\text{SbF}_6)_2$ Prepared Using Method 2. The $[\text{Cu}^{\text{III}}_2(\text{UN-O}^-)(\mu\text{-}\cdot\text{NO})](\text{SbF}_6)_2$ solution was put under vacuum and subsequently purged with argon gas. This process was repeated five times to remove excess $\text{NO}_{(\text{g})}$. Next, 1 mL of $\text{O}_{2(\text{g})}$ was added to the solution, and a distinct change in the UV-vis spectra was observed. The final spectrum of $[\text{Cu}^{\text{III}}_2(\text{UN-O}^-)(\text{OON=O})](\text{SbF}_6)_2$ was recorded at $-80\text{ }^\circ\text{C}$.

Formation of $[\text{Cu}^{\text{III}}_2(\text{UN-O}^-)(\text{OH})](\text{SbF}_6)_2$ by Reaction of $[\text{Cu}^{\text{III}}_2(\text{UN-O}^-)(\text{OON=O})](\text{SbF}_6)_2$ with DTBP. The peroxynitrite complex $[\text{Cu}^{\text{III}}_2(\text{UN-O}^-)(\text{OON=O})](\text{SbF}_6)_2$ can be generated using two methods in DCM, *vide supra*. With either method, adding 1 equiv of DTBP to the peroxynitrite solution at $-80\text{ }^\circ\text{C}$ results in the same spectral change to give $[\text{Cu}^{\text{III}}_2(\text{UN-O}^-)(\text{OH})](\text{SbF}_6)_2$ as the final product, as recorded by UV-vis spectrometry.

Formation and Decay of $[\text{Cu}^{\text{III}}_2(\text{UN-O}^-)(\text{OON=O})](\text{SbF}_6)_2$ in MeTHF as Solvent. First, 1.2 mg (0.001 mmol) of green-color crystalline solid $[\text{Cu}^{\text{III}}_2(\text{UN-O}^-)(\text{DMF})](\text{SbF}_6)_2$ was put in 6 mL of MeTHF in the glovebox. Next, 1.4 mg (0.002 mmol) of KBarF was added to the mixture to help dissolve the solid through anion exchange. The solution mixture was filtered to obtain a clear solution. Next, 3 mL of the clear solution was transferred to a 1 cm path length Schlenk cuvette. The cuvette was placed inside the cell holder of the cryostat and cooled to $-80\text{ }^\circ\text{C}$. The cuvette was left to equilibrate at $-80\text{ }^\circ\text{C}$ for 10 min, after which excess $\text{O}_{2(\text{g})}$ was added to give the dark green spectrum corresponding to $[\text{Cu}^{\text{III}}_2(\text{UN-O}^-)(\text{O}_2^{\cdot-})](\text{SbF}_6)_2$ (Figure 7b). The solution containing $[\text{Cu}^{\text{III}}_2(\text{UN-O}^-)(\text{O}_2^{\cdot-})](\text{SbF}_6)_2$ was put under vacuum and subsequently purged with argon gas. This process was repeated over five cycles to remove excess $\text{O}_{2(\text{g})}$. Next, 0.2 mL of $\text{NO}_{(\text{g})}$ (about 20 equiv) was gradually added to the solution using a gastight three-way syringe. UV-vis spectral changes over the course of 20 min were followed and are depicted as green dotted lines in Figure 7b. Excess $\text{NO}_{(\text{g})}$ was removed using vacuum and argon purge cycles. $[\text{Cu}^{\text{III}}_2(\text{UN-O}^-)(\text{OON=O})](\text{SbF}_6)_2$ (blue spectrum, Figure 7b) was not stable and started to decompose at $-80\text{ }^\circ\text{C}$ (dotted blue lines, Figure 7b). After 1 h, the final spectrum containing $[\text{Cu}^{\text{III}}_2(\text{UN-O}^-)(\text{O}^{2-})]^{2+}(\text{SbF}_6)_2$ and NO_2 was recorded (magenta line, Figure 7b).

Formation of $[\text{Cu}^{\text{III}}_2(\text{UN-O}^-)(\text{OON=O})](\text{SbF}_6)_2$ in MeTHF and Reaction with DTBP. The MeTHF solution of $[\text{Cu}^{\text{III}}_2(\text{UN-O}^-)(\text{OON=O})](\text{SbF}_6)_2$ was generated at $-80\text{ }^\circ\text{C}$, *vide supra*. One equivalent of DTBP was added to the solution after removal of excess $\text{NO}_{(\text{g})}$ using vacuum and argon purge cycles. The reaction product was determined to be $[\text{Cu}^{\text{III}}_2(\text{UN-O}^-)(\text{OH})](\text{SbF}_6)_2$ on the basis of its UV-vis spectral features. The oxidized substrate was analyzed using GC-MS.

Electrospray Ionization Mass Spectrometry (ESI-MS) of $[\text{Cu}^{\text{III}}_2(\text{UN-O}^-)(\text{OON=O})](\text{SbF}_6)_2$. First, 6.1 mg (0.005 mmol) of $[\text{Cu}^{\text{III}}_2(\text{UN-O}^-)(\text{DMF})](\text{SbF}_6)_2$ as a crystalline solid was dissolved in 4 mL of DCM and 1 mL of acetonitrile. The solution was subsequently transferred to a 10 mL Schlenk flask and sealed with rubber septum. The flask was brought out of the glovebox and put in acetone/dry ice cold bath. After allowing the temperature to equilibrate for 10 min, 2 mL of $\text{O}_{2(\text{g})}$ was added to form

$[\text{Cu}^{\text{II}}_2(\text{UN-O}^-)(\text{O}_2^{\bullet-})](\text{SbF}_6)_2$ as a dark green solution. This solution was put under vacuum and then purged with argon gas to remove excess $\text{O}_{2(\text{g})}$. Next, 1 mL of $\text{NO}_{(\text{g})}$ was added to the $[\text{Cu}^{\text{II}}_2(\text{UN-O}^-)(\text{O}_2^{\bullet-})](\text{SbF}_6)_2$ solution, leading the dark green solution to change to a lighter green over the course of 5 min. During this time, the ESI-MS instrument was flushed with -80°C solvent mixture containing 80% DCM and 20% MeCN. Cold solution containing $[\text{Cu}^{\text{II}}_2(\text{UN-O}^-)(^-\text{OON}=\text{O})](\text{SbF}_6)_2$ was injected to the ESI-MS instrument with a gastight syringe, and the mass spectrum was recorded. $[\text{Cu}^{\text{II}}_2(\text{UN-O}^-)(^-\text{OON}=\text{O})](\text{SbF}_6)_2$ was also generated using isotope-labeled $^{18}\text{O}_{2(\text{g})}$, *vide supra*. Identical procedures were followed using the labeled compound, and a mass spectrum was recorded.

Gas Chromatography–Mass Spectrometry (GC-MS) Characterization of Phenol Product. The product mixture from reaction of $[\text{Cu}^{\text{II}}_2(\text{UN-O}^-)(^-\text{OON}=\text{O})](\text{SbF}_6)_2$ with 1 equiv of DTBP in DCM and MeTHF was put on a rotary evaporator to remove the solvent. The solid materials obtained were dissolved using 10 mL of pentane. The solution was filtered through a medium glass-fritted funnel and concentrated to ~ 1 mL for GC-MS tests. The GC-MS conditions for the product analysis were as follows: injector port temperature, 220°C ; detector temperature, 280°C ; column temperature: initial temperature, 120°C ; initial time, 2 min; final temperature, 250°C ; final time, 25 min; gradient rate, $10^\circ\text{C}/\text{min}$; flow rate, 16 mL/min; ionization voltage, 1.5 kV.

Electron Paramagnetic Resonance (EPR) Spectroscopy of Related Complexes. The EPR samples were prepared as follows. First, 4.9 mg (0.004 mmol) of $[\text{Cu}^{\text{II}}_2(\text{UN-O}^-)(\text{DMF})](\text{SbF}_6)_2$ as a crystalline solid was dissolved in 2 mL of DCM in the glovebox to give 2 mL of 2 mM stock solution. Next, 0.5 mL of the stock solution was transferred to a 5 mm o.d. quartz sample tube using a 0.5 mL syringe. This process was repeated three more times to obtain four sample tubes, each containing 0.5 mL of the stock solution. Each of the tubes was sealed with a rubber septum before being taken out of the glovebox. EPR sample preparations and spectra for complex $[\text{Cu}^{\text{II}}_2(\text{UN-O}^-)(\text{DMF})](\text{SbF}_6)_2$ and complex $[\text{Cu}^{\text{II}}_2(\text{UN-O}^-)(\text{O}_2^{\bullet-})](\text{SbF}_6)_2$ were previously published.^{29a}

EPR Spectrum of $[\text{Cu}^{\text{II}}_2(\text{UN-O}^-)(\mu\text{-NO})](\text{SbF}_6)_2$. The EPR sample tubes were placed in a dry ice/acetone bath to maintain the temperature at -80°C . After waiting 10 min for the temperature to equilibrate, 0.2 mL of $\text{NO}_{(\text{g})}$ (about 20 equiv) was gradually added to the solution in one of the tubes using a gastight three-way syringe. The tube was subsequently kept frozen in liquid nitrogen, and the EPR spectrum was taken at 20 K and shown to be silent.

EPR Spectrum of $[\text{Cu}^{\text{II}}_2(\text{UN-O}^-)(^-\text{OON}=\text{O})](\text{SbF}_6)_2$. Complex $[\text{Cu}^{\text{II}}_2(\text{UN-O}^-)(^-\text{OON}=\text{O})](\text{SbF}_6)_2$ was prepared using both of the methods, *vide supra*. The EPR spectra for complexes prepared by both methods were taken at 20 K and shown to be silent.

■ ASSOCIATED CONTENT

● Supporting Information

The Supporting Information is available free of charge on the ACS Publications website at DOI: 10.1021/jacs.6b10689.

Experimental details and data pertaining to various spectroscopies (UV–vis, IR, GC-MS, ESI-MS), including Figures S1–S14 (PDF)

■ AUTHOR INFORMATION

Corresponding Author

*karlin@jhu.edu

ORCID

Kenneth D. Karlin: 0000-0002-5675-7040

Notes

The authors declare no competing financial interest.

■ ACKNOWLEDGMENTS

This work was supported by the National Institutes of Health (NIH) (GM28962 to K.D.K.) and by the National Science Foundation (NSF) (CHE 1254733 to E.K.).

■ REFERENCES

- (1) (a) Campbell, A.; Smith, M. A.; Sayre, L. M.; Bondy, S. C.; Perry, G. *Brain Res. Bull.* **2001**, *55*, 125. (b) Perry, G.; Sayre, L. M.; Atwood, C. S.; Castellani, R. J.; Cash, A. D.; Rottkamp, C. A.; Smith, M. A. *CNS Drugs* **2002**, *16*, 339. (c) Gaggelli, E.; Kozlowski, H.; Valensin, D.; Valensin, G. *Chem. Rev.* **2006**, *106*, 1995.
- (2) (a) Beckman, J. S.; Beckman, T. W.; Chen, J.; Marshall, P. A.; Freeman, B. A. *Proc. Natl. Acad. Sci. U. S. A.* **1990**, *87*, 1620. (b) Beckman, J. S. *Chem. Res. Toxicol.* **1996**, *9*, 836. (c) Beckman, J. S.; Koppenol, W. H. *Am. J. Physiol.* **1996**, *271*, C1424. (d) MacMillan-Crow, L. A.; Crow, J. P.; Thompson, J. A. *Biochemistry* **1998**, *37*, 1613. (e) Radi, R. *Proc. Natl. Acad. Sci. U. S. A.* **2004**, *101*, 4003. (f) Quint, P.; Reutzel, R.; Mikulski, R.; McKenna, R.; Silverman, D. N. *Free Radical Biol. Med.* **2006**, *40*, 453. (g) Pacher, P.; Beckman, J. S.; Liaudet, L. *Physiol. Rev.* **2007**, *87*, 315. (h) Reynolds, M. R.; Berry, R. W.; Binder, L. I. *Biochemistry* **2007**, *46*, 7325. (i) Surlmeli, N. B.; Litterman, N. K.; Miller, A. F.; Groves, J. T. *J. Am. Chem. Soc.* **2010**, *132*, 17174. (j) Jones, L. H. *Chem. Biol.* **2012**, *19*, 1086. (k) Radi, R. *Acc. Chem. Res.* **2013**, *46*, 550. (l) Yu, F.; Li, M.; Xu, C.; Wang, Z.; Zhou, H.; Yang, M.; Chen, Y.; Tang, L.; He, J. *PLoS One* **2013**, *8*, e81526.
- (3) (a) Blough, N. V.; Zafiriou, O. C. *Inorg. Chem.* **1985**, *24*, 3502. (b) Nauser, T.; Koppenol, W. H. *J. Phys. Chem. A* **2002**, *106*, 4084. (c) Goldstein, S.; Lind, J.; Merenyi, G. *Chem. Rev.* **2005**, *105*, 2457.
- (4) (a) Palmer, R. M.; Ferrige, A. G.; Moncada, S. *Nature* **1987**, *327*, 524. (b) Moncada, S.; Palmer, R. M.; Higgs, E. A. *Pharmacol. Rev.* **1991**, *43*, 109. (c) Nathan, C. *FASEB J.* **1992**, *6*, 3051. (d) Garthwaite, J.; Boulton, C. L. *Annu. Rev. Physiol.* **1995**, *57*, 683. (e) Bogdan, C. *Nat. Immunol.* **2001**, *2*, 907.
- (5) (a) Mattson, M. P.; Goodman, Y.; Luo, H.; Fu, W.; Furukawa, K. *J. Neurosci. Res.* **1997**, *49*, 681. (b) Keller, J. N.; Kindy, M. S.; Holtsberg, F. W.; St; Clair, D. K.; Yen, H. C.; Germeyer, A.; Steiner, S. M.; Bruce-Keller, A. J.; Hutchins, J. B.; Mattson, M. P. *J. Neurosci.* **1998**, *18*, 687.
- (6) (a) Ischiropoulos, H.; Beckman, J. S. *J. Clin. Invest.* **2003**, *111*, 163. (b) Valko, M.; Morris, H.; Cronin, M. T. *Curr. Med. Chem.* **2005**, *12*, 1161. (c) Zhu, X.; Su, B.; Wang, X.; Smith, M. A.; Perry, G. *Cell. Mol. Life Sci.* **2007**, *64*, 2202. (d) Uttara, B.; Singh, A. V.; Zamboni, P.; Mahajan, R. T. *Curr. Neuropharmacol.* **2009**, *7*, 65. (e) Kozlowski, H.; Janicka-Klos, A.; Brasun, J.; Gaggelli, E.; Valensin, D.; Valensin, G. *Coord. Chem. Rev.* **2009**, *253*, 2665. (f) Savelieff, M. G.; Lee, S.; Liu, Y.; Lim, M. H. *ACS Chem. Biol.* **2013**, *8*, 856.
- (7) (a) Scheuner, D.; Eckman, C.; Jensen, M.; Song, X.; Citron, M.; Suzuki, N.; Bird, T. D.; Hardy, J.; Hutton, M.; Kukull, W.; Larson, E.; Levy-Lahad, E.; Viitanen, M.; Peskind, E.; Poorkaj, P.; Schellenberg, G.; Tanzi, R.; Wasco, W.; Lannfelt, L.; Selkoe, D.; Younkin, S. *Nat. Med.* **1996**, *2*, 864. (b) Multhaup, G.; Schlicksupp, A.; Hesse, L.; Behr, D.; Ruppert, T.; Masters, C. L.; Beyreuther, K. *Science* **1996**, *271*, 1406. (c) Atwood, C. S.; Scarpa, R. C.; Huang, X.; Moir, R. D.; Jones, W. D.; Fairlie, D. P.; Tanzi, R. E.; Bush, A. I. *J. Neurochem.* **2000**, *75*, 1219.
- (8) (a) Smith, M. A.; Richey Harris, P. L.; Sayre, L. M.; Beckman, J. S.; Perry, G. *J. Neurosci.* **1997**, *17*, 2653. (b) Castegna, A.; Thongboonkerd, V.; Klein, J. B.; Lynn, B.; Markesbery, W. R.; Butterfield, D. A. *J. Neurochem.* **2003**, *85*, 1394. (c) Kummer, M. P.; Hermes, M.; Delekarte, A.; Hammerschmidt, T.; Kumar, S.; Terwel, D.; Walter, J.; Pape, H. C.; König, S.; Roeber, S.; Jessen, F.; Klockgether, T.; Korte, M.; Heneka, M. T. *Neuron* **2011**, *71*, 833.
- (9) (a) Shearer, J.; Szalai, V. A. *J. Am. Chem. Soc.* **2008**, *130*, 17826. (b) Shin, B. K.; Saxena, S. *Biochemistry* **2008**, *47*, 9117. (c) Faller, P.; Hureau, C. *Chem. - Eur. J.* **2012**, *18*, 15910.
- (10) In the A β peptides, the position 10 is a tyrosine residue that is subjected to nitration to form 3-nitrotyrosine.

- (11) Giacomazzi, R.; Ciofini, I.; Rao, L.; Amatore, C.; Adamo, C. *Phys. Chem. Chem. Phys.* **2014**, *16*, 10169.
- (12) (a) Maiti, D.; Lee, D.-H.; Narducci Sarjeant, A. A.; Pau, M. Y. M.; Solomon, E. I.; Gaoutchenova, K.; Sundermeyer, J.; Karlin, K. D. *J. Am. Chem. Soc.* **2008**, *130*, 6700. (b) Park, G. Y.; Deepalatha, S.; Puiuu, S. C.; Lee, D.-H.; Mondal, B.; Narducci Sarjeant, A. A.; del Rio, D.; Pau, M. Y. M.; Solomon, E. I.; Karlin, K. D. *JBIC, J. Biol. Inorg. Chem.* **2009**, *14*, 1301. (c) There are cases in the literature for copper ion, where hydrogen peroxide in some form, reacts with NO_(g) to give peroxyxynitrite chemistry. Mondal and co-workers reported that the nitrosyl adduct of a Cu(II) ligand complex reacts with externally added H₂O₂ to form a reduced metal ion Cu^I-PN complex; Karlin and co-workers found that a LCu^{II}(OOH) complex reacts with NO_(g) to form a LCu^I-PN species. (d) Kalita, A.; Kumar, P.; Mondal, B. *Chem. Commun.* **2012**, 48, 4636. (e) Kim, S.; Siegler, M. A.; Karlin, K. D. *Chem. Commun.* **2014**, 50, 2844. (f) Qiao, L.; Lu, Y.; Liu, B.; Girault, H. H. *J. Am. Chem. Soc.* **2011**, *133*, 19823.
- (13) Wick, P. K.; Kissner, R.; Koppenol, W. H. *Helv. Chim. Acta* **2000**, *83*, 748.
- (14) Kurtikyan, T. S.; Eksuzyan, S. R.; Hayrapetyan, V. A.; Martirosyan, G. G.; Hovhannisyanyan, G. S.; Goodwin, J. A. *J. Am. Chem. Soc.* **2012**, *134*, 13861.
- (15) (a) Schopfer, M. P.; Mondal, B.; Lee, D.-H.; Sarjeant, A. A. N.; Karlin, K. D. *J. Am. Chem. Soc.* **2009**, *131*, 11304. (b) Kurtikyan, T. S.; Ford, P. C. *Chem. Commun.* **2010**, 46, 8570. (c) Kurtikyan and Ford showed that, for a heme complex, this isomerization occurs extremely rapidly, even in a 100 K matrix.
- (16) Richeson, C. E.; Mulder, P.; Bowry, V. W.; Ingold, K. U. *J. Am. Chem. Soc.* **1998**, *120*, 7211.
- (17) (a) Stern, M. K.; Jensen, M. P.; Kramer, K. J. *Am. Chem. Soc.* **1996**, *118*, 8735. (b) Lee, J. B.; Hunt, J. A.; Groves, J. T. *Bioorg. Med. Chem. Lett.* **1997**, *7*, 2913. (c) Haber, A.; Gross, Z. *Chem. Commun.* **2015**, 51, 5812.
- (18) (a) Misko, T. P.; Highkin, M. K.; Veenhuizen, A. W.; Manning, P. T.; Stern, M. K.; Currie, M. G.; Salvemini, D. *J. Biol. Chem.* **1998**, *273*, 15646. (b) Salvemini, D.; Jensen, M. P.; Riley, D. P.; Misko, T. P. *Drug News Perspect.* **1998**, *11*, 204. (c) Shimanovich, R.; Hannah, S.; Lynch, V.; Gerasimchuk, N.; Mody, T. D.; Magda, D.; Sessler, J.; Groves, J. T. *J. Am. Chem. Soc.* **2001**, *123*, 3613. (d) Szabo, C.; Ischiroopoulos, H.; Radi, R. *Nat. Rev. Drug Discovery* **2007**, *6*, 662. (e) Haber, A.; Aviram, M.; Gross, Z. *Chem. Sci.* **2011**, *2*, 295.
- (19) (a) Ford, P. C.; Lorkovic, I. M. *Chem. Rev.* **2002**, *102*, 993. (b) Roncaroli, F.; Videla, M.; Slep, L. D.; Olabe, J. A. *Coord. Chem. Rev.* **2007**, *251*, 1903. (c) Kumar, P.; Lee, Y. M.; Hu, L.; Chen, J.; Park, Y. J.; Yao, J.; Chen, H.; Karlin, K. D.; Nam, W. *J. Am. Chem. Soc.* **2016**, *138*, 7753.
- (20) Clarkson, S. G.; Basolo, F. *Inorg. Chem.* **1973**, *12*, 1528.
- (21) (a) Pfeiffer, S.; Gorren, A. C. F.; Schmidt, K.; Werner, E.; Hansert, B.; Bohle, D. S.; Mayer, B. *J. Biol. Chem.* **1997**, *272*, 3465. (b) Kissner, R.; Koppenol, W. H. *J. Am. Chem. Soc.* **2002**, *124*, 234. (c) Lyman, S. V.; Khairutdinov, R. F.; Hurst, J. K. *Inorg. Chem.* **2003**, *42*, 5259. (d) Koppenol, W. H.; Bounds, P. L.; Nauser, T.; Kissner, R.; Ruegger, H. *Dalton Trans.* **2012**, 41, 13779. (e) Molina, C.; Kissner, R.; Koppenol, W. H. *Dalton Trans.* **2013**, 42, 9898.
- (22) (a) Hughes, M. N.; Nicklin, H. G. *J. Chem. Soc. A* **1970**, 925. (b) Hughes, M. N.; Nicklin, H. G.; Sackrile, W. A. C. *J. Chem. Soc. A* **1971**, 3722. (c) Babich, O. A.; Gould, E. S. *Res. Chem. Intermed.* **2002**, *28*, 575.
- (23) (a) Yokoyama, A.; Han, J. E.; Cho, J.; Kubo, M.; Ogura, T.; Siegler, M. A.; Karlin, K. D.; Nam, W. *J. Am. Chem. Soc.* **2012**, *134*, 15269. (b) Yokoyama, A.; Cho, K. B.; Karlin, K. D.; Nam, W. *J. Am. Chem. Soc.* **2013**, *135*, 14900.
- (24) Yokoyama, A.; Han, J. E.; Karlin, K. D.; Nam, W. *Chem. Commun.* **2014**, 50, 1742.
- (25) Kumar, P.; Lee, Y. M.; Park, Y. J.; Siegler, M. A.; Karlin, K. D.; Nam, W. *J. Am. Chem. Soc.* **2015**, *137*, 4284.
- (26) (a) Herold, S.; Koppenol, W. H. *Coord. Chem. Rev.* **2005**, *249*, 499. (b) Schopfer, M. P.; Wang, J.; Karlin, K. D. *Inorg. Chem.* **2010**, *49*, 6267.
- (27) Su, J.; Groves, J. T. *J. Am. Chem. Soc.* **2009**, *131*, 12979.
- (28) Koebke, K. J.; Pauly, D. J.; Lerner, L.; Liu, X.; Pacheco, A. A. *Inorg. Chem.* **2013**, *52*, 7623.
- (29) (a) Cao, R.; Saracini, C.; Ginsbach, J. W.; Kieber-Emmons, M. T.; Siegler, M. A.; Solomon, E. I.; Fukuzumi, S.; Karlin, K. D. *J. Am. Chem. Soc.* **2016**, *138*, 7055. (b) Mahroof-Tahir, M.; Murthy, N. N.; Karlin, K. D.; Blackburn, N. J.; Shaikh, S. N.; Zubieta, J. *Inorg. Chem.* **1992**, *31*, 3001.
- (30) See [Supporting Information](#).
- (31) Paul, P. P.; Tyeklar, Z.; Farooq, A.; Karlin, K. D.; Liu, S.; Zubieta, J. *J. Am. Chem. Soc.* **1990**, *112*, 2430.
- (32) Fujisawa, K.; Tateda, A.; Miyashita, Y.; Okamoto, K.; Paulat, F.; Praneeth, V. K. K.; Merkle, A.; Lehnert, N. *J. Am. Chem. Soc.* **2008**, *130*, 1205.
- (33) Ruggiero, C. E.; Carrier, S. M.; Antholine, W. E.; Whittaker, J. W.; Cramer, C. J.; Tolman, W. B. *J. Am. Chem. Soc.* **1993**, *115*, 11285.
- (34) Kalita, A.; Deka, R. C.; Mondal, B. *Inorg. Chem.* **2013**, *52*, 10897.
- (35) Wright, A. M.; Wu, G. A.; Hayton, T. W. *J. Am. Chem. Soc.* **2010**, *132*, 14336.
- (36) (a) Silaghi-Dumitrescu, R. *J. Inorg. Biochem.* **2006**, *100*, 396. (b) Ghosh, S.; Dey, A.; Usov, O. M.; Sun, Y.; Grigoryants, V. M.; Scholes, C. P.; Solomon, E. I. *J. Am. Chem. Soc.* **2007**, *129*, 10310.
- (37) Thyagarajan, S.; Incarvito, C. D.; Rheingold, A. L.; Theopold, K. H. *Inorg. Chim. Acta* **2003**, *345*, 333.
- (38) We did attempt to detect the superoxide ligand in [Cu^{II}₂(UN-O⁻)(NO)(O₂)²⁺] (3), employing LT-IR spectroscopy. However, either with ¹⁶O₂ or employing a 1:2:1 ¹⁶O₂:¹⁶O¹⁸O:¹⁸O₂ statistical mixture (which was available), no new bands corresponding to an O-O stretch could be observed. This was also the case for the even more stable complex [Cu^{II}₂(UN-O⁻)(O₂)²⁺] (5). We ascribe either low absorptivity or our instrument cutoff at 1100 cm⁻¹ as the cause. We also attempted resonance Raman spectroscopy on 3; however, this sample was unstable in the laser beam.
- (39) One reviewer suggested that *cis-4*, with a five-membered ring involving the PN ligand, might be strained and therefore unstable. However, we have precedence for similar structural motifs. The superoxide [Cu^{II}₂(UN-O⁻)(μ-1,2-O₂)²⁺] (5, [Chart 1](#)) and the related peroxide complex [Cu^{II}₂(UN-O⁻)(μ-1,2-O₂)²⁺] have been characterized, both existing with μ-1,2-bridging structures (with five-membered ring); see [ref 29a](#) for details.
- (40) Lo, W. J.; Lee, Y. P.; Tsai, J. H. M.; Tsai, H. H.; Hamilton, T. P.; Harrison, J. G.; Beckman, J. S. *J. Chem. Phys.* **1995**, *103*, 4026.
- (41) Tran, N. G.; Kalyvas, H.; Skodje, K. M.; Hayashi, T.; Moenne-Loccoz, P.; Callan, P. E.; Shearer, J.; Kirschenbaum, L. J.; Kim, E. *J. Am. Chem. Soc.* **2011**, *133*, 1184.
- (42) Paul, P. P.; Karlin, K. D. *J. Am. Chem. Soc.* **1991**, *113*, 6331.
- (43) (a) Johnston, H. S.; Graham, R. *Can. J. Chem.* **1974**, *52*, 1415. (b) Harwood, M. H.; Jones, R. L. *J. Geophys. Res.* **1994**, *99*, 22955. (c) Riordan, E.; Minogue, N.; Healy, D.; O'Driscoll, P.; Sodeau, J. R. *J. Phys. Chem. A* **2005**, *109*, 779.
- (44) (a) Laarhoven, L. J. J.; Mulder, P. *J. Phys. Chem. B* **1997**, *101*, 73. (b) Tinberg, C. E.; Lippard, S. J. *Biochemistry* **2010**, *49*, 7902. (c) Shenghur, A.; Weber, K. H.; Nguyen, N. D.; Sontising, W.; Tao, F. M. *J. Phys. Chem. A* **2014**, *118*, 11002.
- (45) Nasir, M. S.; Karlin, K. D.; McGowty, D.; Zubieta, J. *J. Am. Chem. Soc.* **1991**, *113*, 698.
- (46) (a) Barry, S. M.; Kers, J. A.; Johnson, E. G.; Song, L.; Aston, P. R.; Patel, B.; Krasnoff, S. B.; Crane, B. R.; Gibson, D. M.; Loria, R.; Challis, G. L. *Nat. Chem. Biol.* **2012**, *8*, 814. (b) Matthews, M. L.; Chang, W. C.; Layne, A. P.; Miles, L. A.; Krebs, C.; Bollinger, J. M., Jr. *Nat. Chem. Biol.* **2014**, *10*, 209. (c) Dodani, S. C.; Cahn, J. K.; Heinisch, T.; Brinkmann-Chen, S.; McIntosh, J. A.; Arnold, F. H. *ChemBioChem* **2014**, *15*, 2259. (d) Attia, A. A.; Silaghi-Dumitrescu, R. *Int. J. Quantum Chem.* **2014**, *114*, 652. (e) Dodani, S. C.; Kiss, G.; Cahn, J. K.; Su, Y.; Pande, V. S.; Arnold, F. H. *Nat. Chem.* **2016**, *8*, 419.
- (47) The nitric oxide source may be nitrite ion (NO₂⁻) in some of these cases.